ORIGINAL RESEARCH

Prohibitin-1 Is a Dynamically Regulated Blood Protein With Cardioprotective Effects in Sepsis

Taylor A. Mattox, PhD*; Christine Psaltis [iD], PhD*; Katie Weihbrecht, PhD; Jacques Robidoux [iD], PhD; Brita Kilburg-Basnyat [iD], PhD; Michael P. Murphy, PhD; Kymberly M. Gowdy [iD], PhD; Ethan J. Anderson [iD], PhD

BACKGROUND: In sepsis, circulating cytokines and lipopolysaccharide elicit mitochondrial dysfunction and cardiomyopathy, a major cause of morbidity and mortality with this condition. Emerging research places the PHB1 (lipid raft protein prohibitin-1) at the nexus of inflammation, metabolism, and oxidative stress. PHB1 has also been reported in circulation, though its function in this compartment is completely unknown.

METHODS AND RESULTS: Using a wide-ranging approach across multiple in vitro and in vivo models, we interrogated the functional role of intracellular and circulating PHB1 in the heart during sepsis, and elucidated some of the mechanisms involved. Upon endotoxin challenge or sepsis induction in rodent models, PHB1 translocates from mitochondria to nucleus in cardiomyocytes and is secreted into the circulation from the liver in a manner dependent on nuclear factor (erythroid-derived 2)-like 2, a key transcriptional regulator of the antioxidant response. Overexpression or treatment with recombinant human PHB1 enhances the antioxidant/anti-inflammatory response and protects HL-1 cardiomyocytes from mitochondrial dysfunction and toxicity from cytokine stress. Importantly, administration of recombinant human PHB1 blunted inflammation and restored cardiac contractility and ATP production in mice following lipopolysaccharide challenge. This cardioprotective, anti-inflammatory effect of recombinant human PHB1 was determined to be independent of nuclear factor (erythroid-derived 2)-like 2, but partially dependent on PI3K/AKT signaling in the heart.

CONCLUSIONS: These findings reveal a previously unknown cardioprotective effect of PHB1 during sepsis, and illustrate a pro-survival, protective role for PHB1 in the circulation. Exploitation of circulating PHB1 as a biomarker and/or therapeutic could have widespread benefit in the clinical management of sepsis and other severe inflammatory disorders.

Key Words: cardiomyopathy ■ circulating factor ■ inflammation ■ mitochondria ■ prohibitins ■ redox ■ shock

Overwhelming inflammatory stress imposed by circulating cytokines during the acute phase response in sepsis often precipitates rapid collapse of organ function, particularly within the cardiovascular system, where myocardial depression is associated with an ≈3-fold increased risk of mortality.[1–3] Efforts to identify the signals that govern the duration and magnitude of inflammatory stress during sepsis have

uncovered novel pathways involving lipid mediators (eg, resolvins, protectins), small peptides, oligonucleotides, neurohumoral factors, and others.[4,5] Previous studies have also shown that pro-inflammatory cytokines lead to myocardial depression in sepsis, at least in part, via their deleterious impact on mitochondrial energetics.[6–11] Unfortunately, although they have provided mechanistic insight, these studies have not

CLINICAL PERSPECTIVE

What Is New?

- We have discovered that the PHB-1 (lipid raft scaffold protein prohibitin 1) is abundant in blood and behaves like an acute phase reactant protein during sepsis.
- Hepatocytes are a major source of circulating PHB1 and its secretion, but not expression, is regulated by transcription factor nuclear factor erythroid 2-related factor 2.
- PHB1 overexpression or treatment with recombinant human PHB-1 preserves mitochondrial oxidative phosphorylation and upregulates antioxidant capacity in cardiomyocytes undergoing inflammatory stress; dosing mice with recombinant human PHB-1 blunts inflammation and induces pro-survival signaling in heart, in part via PI3KAKT signaling.

What Are the Clinical Implications?

- Circulating levels of PHB1 may be useful as a biomarker of cardiac and/or organ dysfunction in patients with sepsis.
- Exploiting the pro-survival, cardioprotective effect of PHB1 provides a blueprint for development of novel therapies to treat inflammatory disorders.

Nonstandard Abbreviations and Acronyms

Nrf2	nuclear factor (erythroid-derived 2)-like 2
PHB1/2	prohibitin 1/2
ROS	reactive oxygen species

translated into new therapies to combat organ dysfunction in sepsis, and mortality for patients in septic shock remains as high today (≈30%) as it was several decades ago.[12,13]

PHB1 and PHB2 (prohibitins) are proteins that assemble in hetero-oligomeric complexes within the mitochondrial inner membrane and in plasma membrane lipid rafts where they play critical roles in mitochondrial function and metabolism,[14–18] cellular proliferation and tumorigenesis,[19–21] inflammation/oxidative stress,[22] and apoptosis.[23–25] Little information exists regarding the function of PHBs in the heart, although overexpression of PHB1 was shown to protect against oxidative insults in cardiomyocytes.[26,27] PHB1 has antioxidant and protective effects in colonic epithelium,[28] effects that are accompanied by sustained activation of the nuclear factor erythroid 2-related factor 2 (Nrf2), a key

transcriptional regulator of the antioxidant response system.[29] There is evidence that PHBs are in the circulation, with 1 report showing that PHB1 is capable of binding to and activating complement,[30] while others have documented the presence of PHB1/2 in serum of patients with cancer.[31–33] Despite these reports, the function of PHBs in the circulation is completely unknown.

Since PHB1 is known to have pleiotropic protective effects, and because prior reports have outlined a role for this protein in regulating inflammation, we sought to determine the extent to which PHB1 regulates inflammation and metabolism in the heart during sepsis, and the mechanisms by which it may be acting. Our findings uncover a previously unrecognized role for PHB1 as a dynamically regulated circulatory protein that has pro-survival, cardioprotective effects when administered as a recombinant biologic therapy in sepsis.

METHODS

A detailed and expanded description of all methods and materials used in this study, including Tables of primers for quantitative real-time polymerase chain reaction and antibodies used for protein detection and immunocytochemistry, is included in Data S1. All data related to the findings of this study are available from the corresponding author upon request.

Experimental Animals

All experiments in rodent models were conducted with approval from the Institutional Animal Care and Use Committee at East Carolina University and the University of Iowa, in accordance with the National Institutes of Health *Guide for the Care and Use of Laboratory Animals*. Male Sprague-Dawley rats (Charles River Laboratory, Wilmington, MA) weighing between 275 and 300 g (14–16 weeks old), and C57/Bl6J wild-type (WT) mice (The Jackson Laboratory, Sacramento, CA) weighing between 20–25 grams (8–10 weeks old) were used. The Nrf2$^{-/-}$ mice on a C57/Bl6J background were a kind gift from Thomas Kensler. Animals were housed in temperature- and light-controlled conditions with free access to food and water. Unless otherwise specified, animals were deeply anesthetized with pharmaceutical grade ketamine (80–100 mg/kg) and xylazine (10–12.5 mg/kg), before euthanasia via exsanguination and cardiac dissection.

Primary Hepatocyte Isolation

Primary hepatocytes were isolated from WT and Nrf2$^{-/-}$ mice according to procedures outlined previously[34,35] and described in detail in Data S1.

Induction of Endotoxemia and Dosing of Recombinant Human PHB1

Male rats (N=6 per group) and mice (N=8 per group) were given an intraperitoneal injection of lipopolysaccharide purified from *Escherichia coli* (Sigma-Aldrich, St. Louis, MO) mixed in 5% dextrose-H_2O at various concentrations [rats: 0.5 and 7.5 mg/kg and mice: 12 mg/kg]. The control group received an injection of 5% dextrose-H_2O (Vehicle). Following the lipopolysaccharide injection, all animals were monitored every 4 hours until euthanasia. Approximately 25% of the animals in the lipopolysaccharide groups succumbed to shock and/or were euthanized for humane reasons before completion of the experiments. Purified recombinant human PHB1 (Origene, Rockville, MD) was diluted in saline immediately before injection. Mice received an intraperitoneal injection of recombinant PHB1 (rPHB1) (300 ng, corresponding to 9–10 µg/kg body weight) to achieve a final circulating concentration of 200 ng/mL at +2, +8, and +14 hours following lipopolysaccharide challenge. This concentration of rPHB1 was estimated by assuming a mouse blood volume/mass ratio of 58.5 mL/kg.[36] For studies with the phosphoinositide-3 kinase (PI3K) inhibitor buparlisib, mice were injected with buparlisib (30 mg/kg body weight) dissolved in 100 µL of the vehicle (0.1 M sulfobutylether-β-cyclodextrin, SBE-β-CD, MedChemExpress, in ddH_2O) 1 hour before lipopolysaccharide challenge. Vehicle-treated mice were treated with the SBE-β-CD alone before lipopolysaccharide. Dosing of rPHB1 was then administered in these mice as described above.

Induction of Sepsis Via Cecal Ligation and Puncture

Male C57/Bl6J mice (N=8 per group, WT) were anesthetized under 2%–3% vaporized isoflurane in oxygen at a flow rate of 100 mL/min. The abdomen was shaved and prepped with Hibiclens followed by 70% isopropanol to sterilize the surgical field. Bupivacaine was applied topically to skin before incision. A surgical drape was made with Press & Seal Wrap and a fenestration cut to allow access to the incision site. A 5–8-mm horizontal incision was made in the abdomen, and the cecum was identified and pulled out slightly from the cut muscle/skin. Ligation of the ileocecal junction was made with 4–0 silk suture. The cecum was punctured proximal to the ligation with a 27G needle and a small amount of cecal contents was allowed to spill out. Cecum was then returned to the abdomen and the incision was closed using silk suture and Vetbond. Sham animals underwent a similar procedure: laparotomy as described above with no cecal ligation or puncture. A bolus of 1 mL saline was then injected subcutaneously for fluid support, and animals were allowed to recover from surgery under a heat lamp and

monitored for up to 48 hours, with cohorts being euthanized at time points indicated in Figure 1 under ketamine/xylazine as described above. Approximately 30% of the animals in the cecal ligation and puncture groups succumbed to shock and/or were euthanized for humane reasons before completion of the experiments.

Echocardiography

Echocardiography in rats, WT, and Nrf2$^{-/-}$ mice outlined in experiments shown in Figures 1, 3 and 4 were performed under controlled anesthesia (2%–3% vaporized isoflurane in oxygen at a flow rate of 100 mL/min) using a 30 MHz transducer (Vevo 2100, VisualSonics, Toronto, ON). Cardiac functional parameters were recorded at baseline, +4, and +24 hours following lipopolysaccharide in the rat model and at baseline, +4, +8, and +14 hours following lipopolysaccharide in the mouse model. Echocardiography in the mice used in buparlisib experiments was performed on conscious mice 16 hours following lipopolysaccharide challenge, by staff in the cardiovascular phenotyping core facility at University of Iowa.

Mitochondrial Function in Permeabilized Left Ventricular Myofibers and HL-1 Cardiomyocytes

Mitochondrial O_2 consumption, ATP production, Ca^{2+} uptake, and H_2O_2 emission were measured in permeabilized left ventricular myofibers and HL-1 cardiomyocytes according to previously published protocols from our group,[37–41] and described in detail in Data S1.

Statistical Analysis

Statistical analysis was performed with PRISM (GraphPad, San Diego, CA). All data are expressed as means ± standard error of the mean (SEM) unless otherwise noted. For cell culture models, a 2-way ANOVA (transfection × treatment) followed by Tukey's post hoc multiple comparisons test was used to test for main effect of cytokine treatment between groups. For rodent models, student's *t* test (two-tail) or 1-way ANOVA followed by Tukey's test was used to test for differences in main effect of lipopolysaccharide and rPHB1 treatment between groups within each genotype, as described in each of the Figure legends. In all cases, $P<0.05$ indicated statistically significant differences between groups.

RESULTS

Dynamic Changes in PHB1 Levels in the Heart and Blood During Sepsis

Cardiac electromechanical dysfunction is a well-described complication of severe sepsis, including
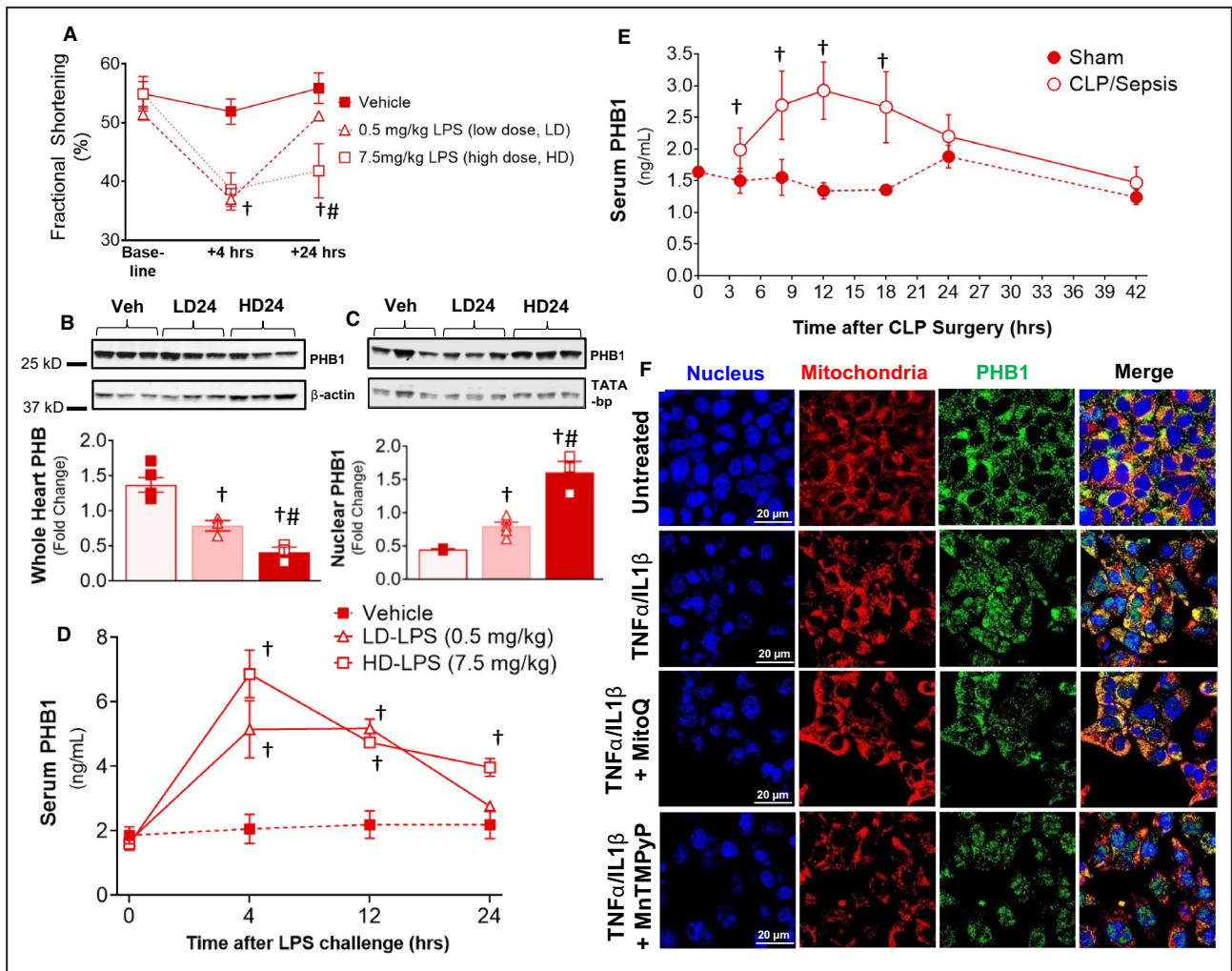
Figure 1. PHB1 mobilizes within the heart and circulation during sepsis.
Endotoxemia was induced in Sprague-Dawley rats with both low-dose (0.5 mg/kg, LD) and high-dose (HD) LPS (7.5 mg/kg, HD), and cardiac function parameters (fractional shortening) was assessed in the rats at +4 and +24 hours (**A**). Total levels of PHB1 protein were assessed in whole heart (**B**) and nuclear fraction of the heart (**C**), and in the serum (**D**) of the rats at time points indicated following LPS challenge. Serum PHB1 levels in mice at time points following CLP-induced sepsis is indicated in (**E**). Localization of endogenous PHB1 in HL-1 cardiomyocytes following a 4-hour exposure to sepsis-mimetic concentration of TNFα/IL1β, with or without the mitochondrial-targeted antioxidant MitoQ, or the nontargeted free radical scavenger MnTMPyP, is shown in (**F**). N=4 rats/group for LPS experiments, N=7–10 mice per group for CLP. A 2-tail Student t test was used to compare main effect of LPS or CLP vs Vehicle or Sham control, respectively, at each time point. †$P<0.01$ vs Vehicle or Sham, #$P<0.001$ vs low-dose LPS for that respective time point/condition. LD4, low-dose LPS at 4 hours postinjection, LD24, low-dose LPS at 24 hours postinjection; HD24, high-dose LPS at 24 hours postinjection. CLP indicates cecal ligation and puncture; .IL1β, interleukin 1β; LPS, lipopolysaccharide; PHB, prohibitin; TNFα, tumor necrosis factor α; and Veh, vehicle.

both systolic and diastolic dysfunction.[1,2] A classic experimental model of severe sepsis involves injection of lipopolysaccharide at sufficiently high dose to elicit myocardial depression and the "cytokine storm." We first examined cardiac PHB1 in the context of severe sepsis using lipopolysaccharide at 2 doses—a low, sublethal (0.5 mg/kg, LD) and high, lethal dose (7.5 mg/kg, HD), in Sprague-Dawley rats. As expected, both doses of lipopolysaccharide caused a sharp decrease in systolic function within 4 hours, which was sustained in the HD group at 24 hours

following lipopolysaccharide injection (Figure 1A). Derangements in mitochondrial function were also present at both doses, with decreased respiration and elevated reactive oxygen species (ROS) production (Figure S1). Cardiac PHB1 in whole tissue lysates decreased in a dose-dependent manner with lipopolysaccharide (Figures 1B), but the remaining PHB1 accumulated in the nucleus (Figures 1C). Interestingly, circulating PHB1 levels were highly dynamic in the acute phase following lipopolysaccharide challenge at both doses, showing peak elevations in serum at
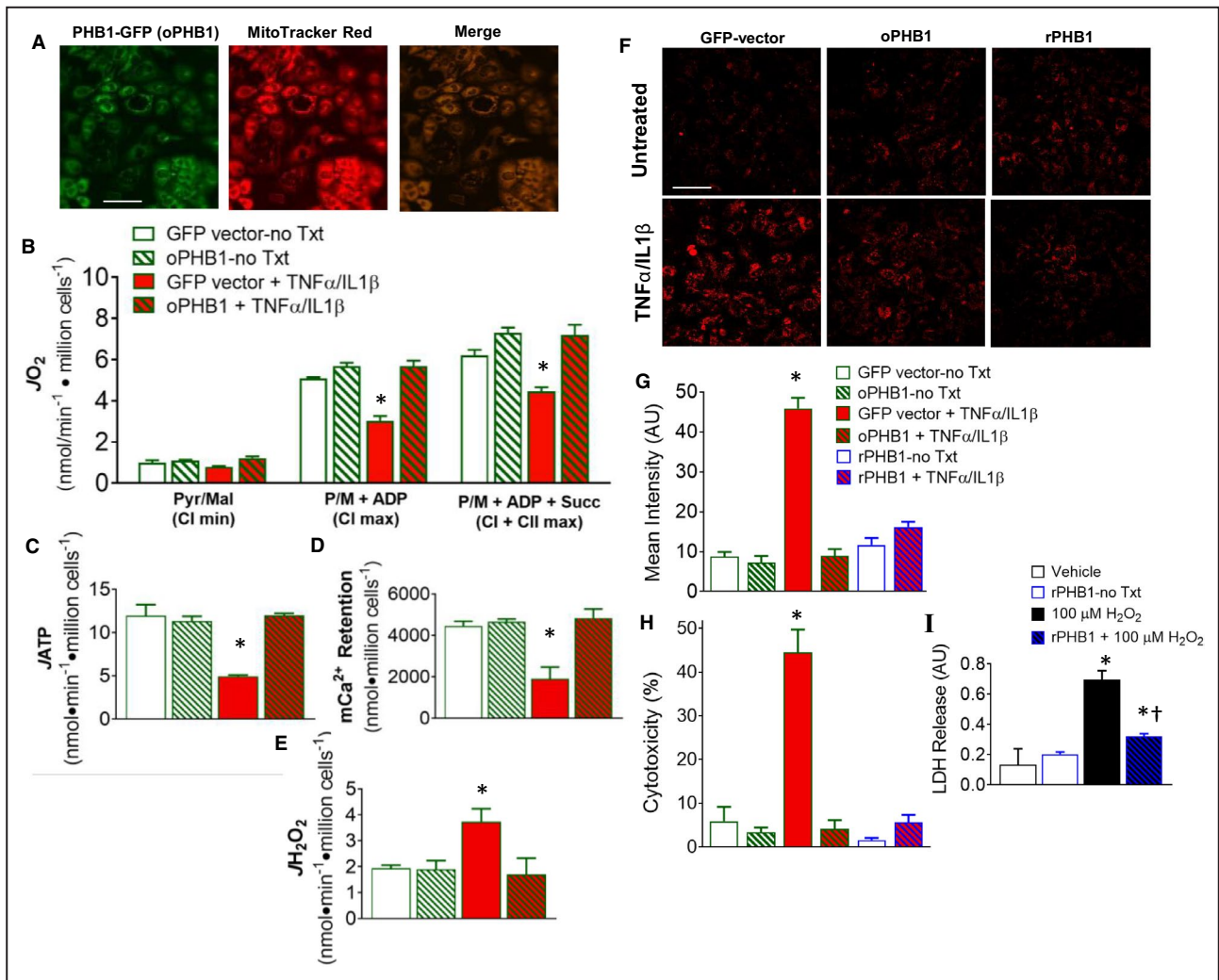
Figure 2. PHB1 preserves mitochondrial energetics and viability during inflammatory and oxidative stress in HL-1 cardiomyocytes.

Cells were transiently transfected with plasmid DNA containing PHB1-GFP for 24 hours, then labeled with MitoTracker Red to confirm mitochondrial localization (**A**). The mitochondrial-protective effect of overexpressing PHB1 (oPHB1) in HL-1 cardiomyocytes exposed to TNFα/IL1β (**B**) is illustrated with respiratory flux (J-O_2) supported by pyruvate/malate (complex I substrate, CI), or pyr/mal + succinate (CI and CII substrates), ATP production (JATP) with pyruvate/malate (Pyr/Mal) (**C**), Ca^{2+} sensitivity of permeability transition pore (**D**), and H_2O_2 production/emission (**E**). Representative images of mitochondrial ROS staining with MitoSox in HL-1 cardiomyocytes exposed to a sepsis-mimetic concentration of TNFα/IL1β in GFP-vector control, oPHB1 and with recombinant human PHB1 (rPHB1) is shown in (**F**) and quantified in (**G**). Cytotoxicity was assessed by LDH release in HL1 cardiomyocytes following exposure to TNFα/IL1β (**H**) and H_2O_2 (**I**). For oPHB1 experiments, N=3–4 with technical replicates for each condition. A 2-way ANOVA (transfection × treatment) followed by Tukey's post hoc multiple comparisons test was used to compare main effect of cytokine treatment on end points indicated. *$P<0.0001$ vs untreated, GFP-vector Control. For gene expression and cytotoxicity analysis, N=4 per group with technical replicates for each condition. *$P<0.0001$ vs untreated Control, †$P<0.0001$ vs TNFα/IL1β, or H_2O_2 treated groups. AU indicates arbitrary units ; GFP, green fluorescent protein; IL1β, interleukin 1 β; LDH, lactate dehydrogenase; P/M, Pyruvate/Malate; ROS, reactive oxygen species; and TNFα, tumor necrosis factor α.

4 to 12 hours post-lipopolysaccharide (Figure 1D). To determine whether this elevation in serum PHB1 was exclusive to lipopolysaccharide challenge and/or the rat model, we used cecal ligation-puncture to induce severe sepsis in WT mice and observed a time-dependent rise and fall of serum PHB1 that followed a very similar time course to the endotoxemia model in the rats (Figure 1E).

In order to more closely delineate the factors regulating the mobilizability of PHB1 in the heart during sepsis, we developed an in vitro model of acute inflammatory stress using a sepsis-mimetic cocktail of the pro-inflammatory cytokines tumor necrosis factor/interleukin-1β (TNFα/IL-1β) in HL-1 cardiomyocytes (Figure S2). Just as was observed in the rat heart following lipopolysaccharide challenge, a similar
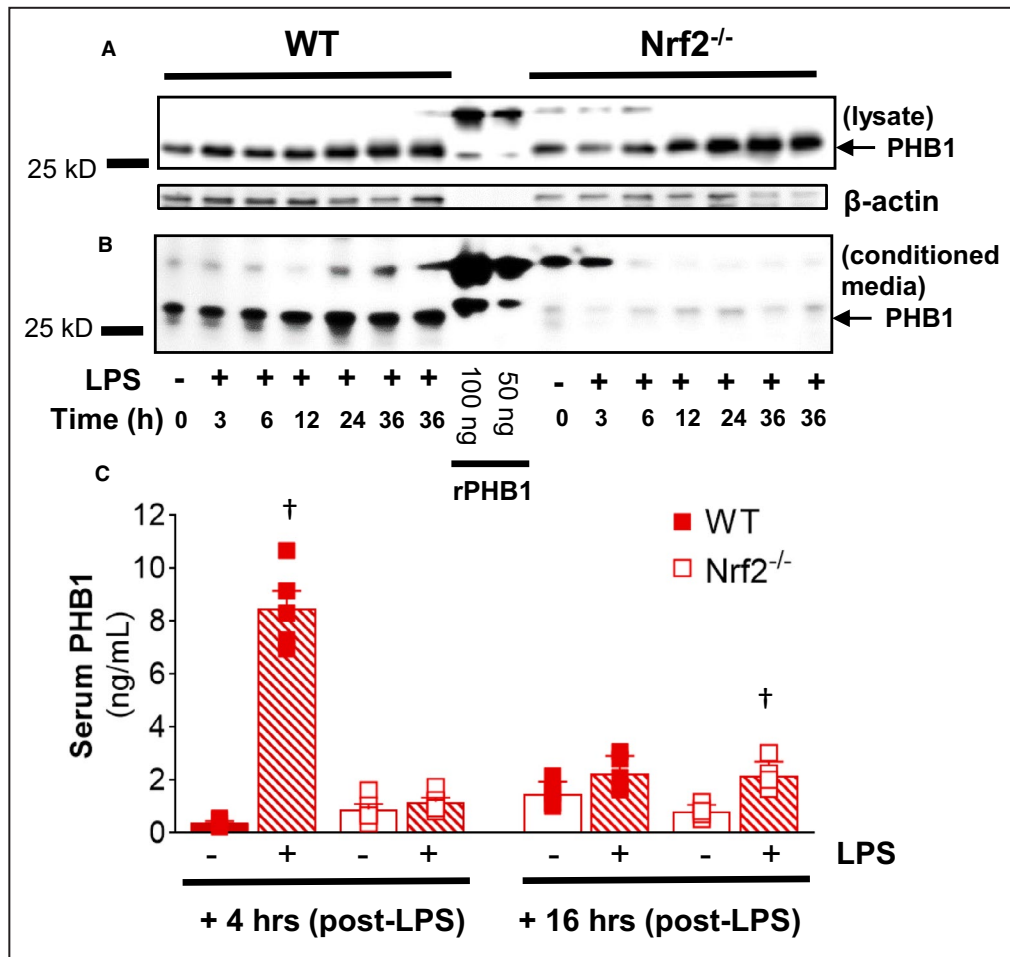
Figure 3. Endotoxin-induced secretion of PHB1 in liver is dependent on Nrf2.
Shown in (**A**) is a representative immunoblot of PHB1 in whole cell lysates, and in the conditioned media (**B**) obtained from primary murine hepatocytes exposed to LPS (2.5 ng/mL) for the time points indicated. Serum PHB1 from WT and Nrf2$^{-/-}$ mice at +4 hours and +16 hours following a 12 mg/kg dose of LPS is shown in (**C**). Blots are representative of 2 independent experiments in hepatocytes. For mouse model serum PHB1, N=5. A 2-tail Student t test was used to compare main effect of LPS vs vehicle control for each genotype at each time point. †$P<0.05$ vs control (vehicle-treated) mice. LPS indicates lipopolysaccharide; Nrf2, nuclear factor (erythroid-derived 2)-like 2; rPHB1, recombinant human prohibitin 1; and WT, wild type.

mitochondria-to-nucleus translocation of PHB1 occurred in HL-1 cardiomyocytes in response to a 4-hour treatment with TNFα/IL-1β. This nuclear translocation of PHB1 was significantly blunted by the mitochondrial lipid peroxide-scavenger Mito-quinone, although a cell-permeable superoxide-radical scavenger (MnTMPyP) had no effect (Figure 1F) and was much less effective at blunting the nuclear translocation.

PHB1 Protects HL-1 Cardiomyocytes From Inflammatory Stress Via Preservation of Mitochondrial Function and Upregulation of Antioxidant Capacity

Previous studies have reported that PHB1 protects cells against various stressors, including oxidative

stress and inflammation.[22,28,42] To examine whether PHB1 is acting in similar manner during acute inflammation, HL-1 cardiomyocytes were transfected with plasmid encoding PHB1 with a GFP (green fluorescent protein) tag under control of CMV promoter (overexpression of PHB1), or GFP vector alone (Vec). As expected, localization of PHB1-GFP in normal, unstressed HL-1 cardiomyocytes was primarily mitochondrial (Figure 2A). Overexpression of PHB1-GFP in these cells did not alter mitochondrial function, but did attenuate the deleterious effects of TNFα/IL-1β on mitochondrial respiration, ATP production, ROS production, and Ca^{2+}-sensitization of the permeability transition pore (Figure 2B through 2F), supporting a role for PHB1 in preserving mitochondrial function and integrity under inflammatory stress.
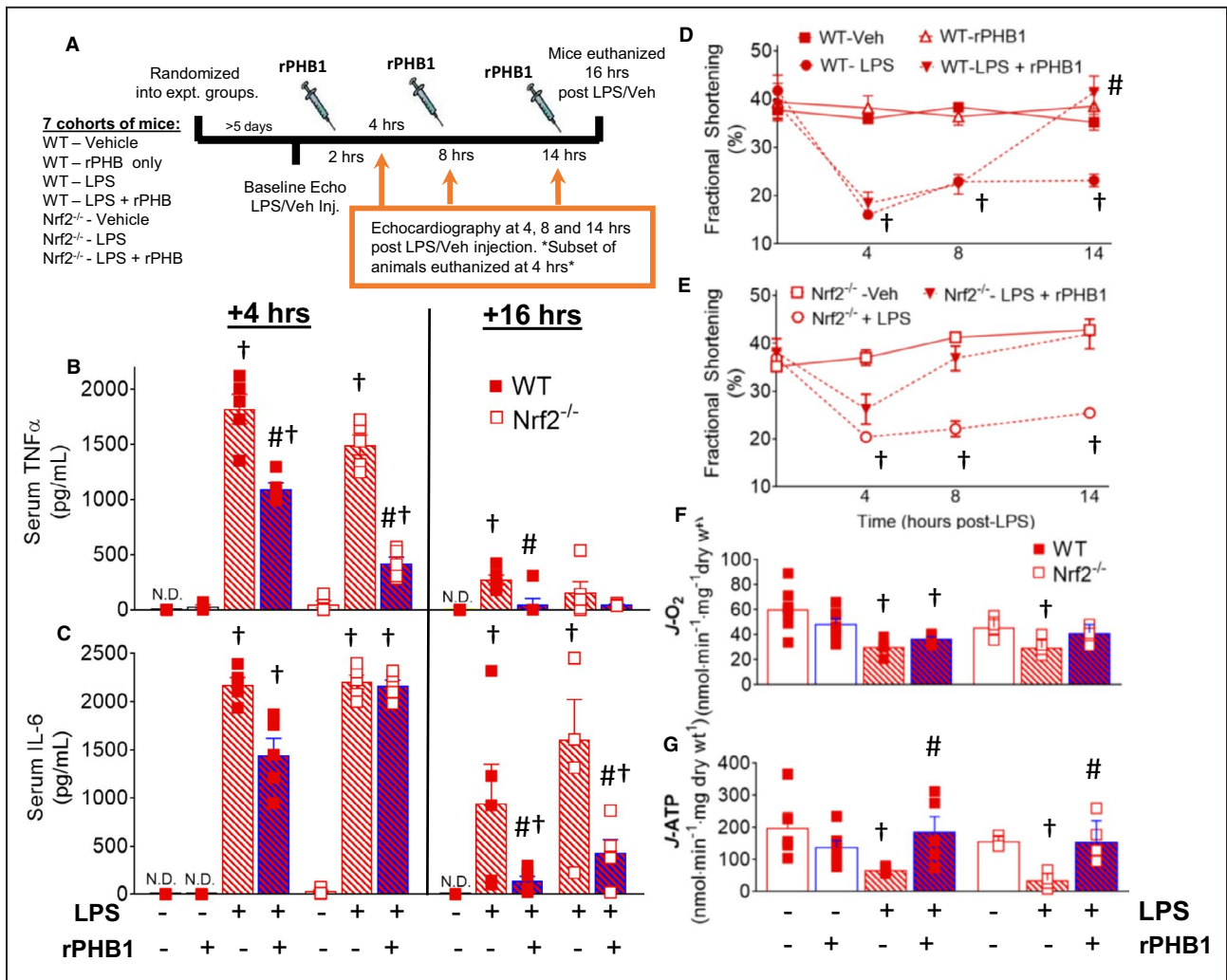
Figure 4. Administration of rPHB1 restores cardiac systolic function and mitochondrial OxPHOS during endotoxemia independent of Nrf2.

The broad experimental design and mouse genotypes/treatment groups is outlined in (**A**). Serum concentrations of TNFα (**B**) and IL-6 (**C**) were measured in WT and Nrf2−/− mice +4 hours and +16 hours after LPS challenge in mice administered either saline vehicle (red-shaded bars), or rPHB1 (blue-shaded bars) at +4, 10 and +16 hours after LPS challenge. Cardiac systolic function in WT (**D**) and Nrf2−/− mice (**E**) were determined in response to LPS challenge and administration of vehicle or rPHB1 at time points indicated. Rates of pyruvate/malate (CI) -supported mitochondrial respiration (J-O$_2$) (**F**) and ATP production (J-ATP) (**G**) in permeabilized ventricular myofibers prepared from the mice at +16 hours are also shown. N=4–6 mice in each group. A 1-way ANOVA followed by Tukey's post hoc multiple comparisons test between groups was used to test for differences in main effect of LPS and rPHB1 treatment within each genotype. †$P<0.05$ vs untreated mice (- LPS, -rPHB1), and #$P<0.05$ vs +LPS for that respective time point and genotype. LPS indicates lipopolysaccharide; N.D., not detectable; Nrf2, nuclear factor (erythroid-derived 2)-like 2; OxPHOS, oxidative phosphorylation; rPHB1, recombinant human prohibitin 1; TNFα, tumor necrosis factor α; and WT, wild type.

Overexpression of PHB1 was shown in a prior report to protect cardiomyocytes against oxidative stress in prior studies, although the mechanisms of protection were not clearly determined.[26,27] Interestingly, recombinant human PHB1 (rPHB1) protected pancreatic cells against oxidative stress induced by ethanol,[22] suggesting that PHB1 also acts via exogenous mechanisms. To gain mechanistic insight into these protective effects of PHB1, HL-1 cardiomyocytes were transfected with a lentiviral-based reporter system containing tandem repeats of the antioxidant response element promoter controlling expression of GFP. Cells treated with rPHB1 exhibited robust activation of antioxidant response element promoter, even in the presence of TNFα/IL-1β (Figure S3A and S3B). Moreover, both overexpression of PHB1 and rPHB1-treated cells had increased nuclear localization of the antioxidant response element transcriptional activator Nrf2 (not shown) and upregulation of antioxidant/ phase II detoxifying genes (Figure S3C). In parallel with this upregulation of antioxidant enzymes, overexpression of PHB1 and rPHB1 abrogated inflammatory

gene expression in HL-1 cardiomyocytes following stimulation with TNFα/IL-1β (Figure S4). These anti-oxidant/anti-inflammatory effects of PHB1 were indeed cytoprotective, as overexpression of PHB1 and rPHB1 mitigated mitochondrial ROS (Figure 2F and 2G), and cytotoxicity induced by overnight exposure to TNFα/IL-1β (Figure 2H) and H_2O_2 (Figure 2I).

Endotoxin-Induced Secretion of PHB1 Is Mediated by Nrf2 in Hepatocytes

A principal source of acute phase proteins during sepsis is the liver.[43,44] Additionally, Nrf2 is known to have a key role in regulating the innate immune response to sepsis, and Nrf2^{−/−} mice are more susceptible to sepsis-induced injury and mortality as compared with WT mice.[45] Given that rPHB1 has a potent cytoprotective effect, we sought to determine whether hepatocytes are a potential source of blood-borne PHB1 and whether expression and/or secretion of PHB1 is dependent on Nrf2. Both intracellular and extracellular (in conditioned media) PHB1 increased dramatically in primary hepatocytes from WT mice in time-dependent manner following exposure to low, sublethal dose (2.5 ng/mL) of lipopolysaccharide (Figure 3A and 3B). Surprisingly, in Nrf2^{−/−} hepatocytes, upregulation of PHB1 expression occurred to similar or slightly greater extent than in WT, but secretion of PHB1 was almost completely abrogated. Moreover, this effect was reproducible in mice following lipopolysaccharide challenge, whereby serum PHB1 levels increased considerably at 4 hours following lipopolysaccharide in WT mice, but not in Nrf2^{−/−} mice (Figure 3C), although a very modest increase above baseline was observed in the Nrf2^{−/−} mice 16 hours after lipopolysaccharide.

Intraperitoneal Dosing of rPHB1 Suppresses Inflammation and Preserves Mitochondrial Energetics and Cardiac Function During Endotoxemia Independent of Nrf2

Given the anti-inflammatory and cytoprotective effects of rPHB1 seen in the cardiomyocytes, we next examined whether these protective effects of rPHB1 also occur in vivo during endotoxemia, and whether these effects are dependent on Nrf2. Both WT and Nrf2^{−/−} mice were given an intraperitoneal injection of a high dose of lipopolysaccharide (12 mg/kg b.w.), then 3 doses of rPHB1 (300 ng, corresponding to 9–10 μg/kg b.w.) were administered to the mice via intraperitoneal injection at +2, +8, and +14 hours following lipopolysaccharide. Echocardiography was performed at 3 time points following lipopolysaccharide, immediately after the 3 intraperitoneal doses of rPHB1 each

animal received, and a subset of mice were euthanized 2 hours after the first rPHB1 injection for analysis (Figure 4A).

Dosing of rPHB1 following lipopolysaccharide injection triggered a rapid and systemic anti-inflammatory effect. Serum TNFα levels were diminished in both WT and Nrf2^{−/−} mice by just a single dose of rPHB1 at 4 hours, and were completely back to normal after 3 doses of rPHB1 at 16 hours (Figure 4B). A similar effect of rPHB1 on circulating IL-6 was observed, although a single dose of rPHB1 had no effect on circulating IL-6 in the Nrf2^{−/−} mice (Figure 4C). Importantly, dosing of rPHB1 led to improvements in cardiac function. Every animal that received rPHB1 after lipopolysaccharide challenge had systolic function and other major hemodynamic parameters return to normal by 16 hours following lipopolysaccharide (Figure 4D and 4E and Table). This cardioprotective effect occurred to similar extent in both WT and Nrf2^{−/−} mice, and may even have been more rapid in the Nrf2^{−/−} mice than in WT, suggesting the cardioprotective effect of rPHB1 is independent of Nrf2.

We also assessed the effect of rPHB1 on mitochondrial respiration and ATP production during endotoxemia using permeabilized left ventricular myofibers prepared from WT and Nrf2^{−/−} mice after the third dose of rPHB1 (16 hours post-lipopolysaccharide). Maximal ADP-stimulated respiration in both WT and Nrf2^{−/−} mice was diminished by lipopolysaccharide and was unaffected by rPHB1 (Figure 4F and Figure S5). However, ATP production rates were significantly improved with rPHB1 in both WT and Nrf2^{−/−} mice (Figure 4G), suggesting that rPHB1 may have a specific effect on the mitochondrial phosphorylation system.

The anti-inflammatory effect of rPHB1 was also observed in the myocardium of both WT and Nrf2^{−/−} mice, as nuclear activation of the pro-inflammatory transcription factors nuclear factor κ light-chain-enhancer of activated B cells and phospho-signal transducer and activator of transcription 3 (Tyr705), and pro-inflammatory gene markers were blunted in the heart after just a single dose of rPHB1 (Figure 5). To ascertain whether the anti-inflammatory effects of rPHB1 were limited to the heart, we measured expression of pro-inflammatory cytokines in liver, kidney, and lungs in the WT mice after 3 successive doses of rPHB1. Treatment with rPHB1 suppressed lipopolysaccharide-induced TNFα expression only in kidney tissue (Figure S6A), while rPHB1 completely blunted lipopolysaccharide-induced IL-6 expression in liver, kidney, and lung tissue (Figure S6B). Lipopolysaccharide-induced IL-1β expression was not affected by rPHB1 in any tissues (Figure S6C). We also assessed markers of tissue damage and necrosis in a subset of the mice. As expected, lipopolysaccharide challenge increased circulating lactate dehydrogenase (LDH) and NADH

Table. Cardiac Function Parameters for WT and Nrf2−/− Mice With Endotoxemia

	WT										Nrf2−/−						
	Veh	rPHB1 only			LPS only			rPHB1 +LPS			Veh	LPS only			rPHB1 +LPS		
		4 h	8 h	14 h	4 h	8 h	14 h	4 h	8 h	14 h		4 h	8 h	14 h	4 h	8 h	14 h
Age, wks	11.60±0.5	12.25±1.0			11.60±0.5			12.33±0.8			9.50±0.7	9.25±0.5			9.50±0.6		
Weight, g	26.16±2.3	27.60±2.0			26.96±1.0			26.65±1.3			24.35±1.5	23.96±1.0			24.20±1.6		
LVeSD, mm	2.53±0.3	2.46±0.4	2.53±0.3	2.39±0.4	3.49±0.4*	3.01±0.2*	3.19±0.3*	3.29±0.3*	3.15±0.4*	2.12±0.5	2.65±0.3	3.24±0.2*	3.03±0.3*	2.79±0.3	2.82±0.1	2.33±0.2	2.11±0.5
LVeDD, mm	3.99±0.3	3.95±0.4	3.97±0.3	3.86±0.3	4.16±0.4	3.90±0.2	4.14±0.3	4.03±0.2	4.05±0.2	3.57±0.4	4.34±0.3	4.07±0.2	3.88±0.3	3.75±0.3	3.84±0.3	3.69±0.2	3.77±0.3
Heart rate, bpm	463.98±42.6	531.14±24.1	526.04±28.9	505.99±35.1	552.34±40.8*	459.69±22.4	412.35±52.3	565.26±36.0*	497.13±57.9	482.52±46.4	435.33±40.1	527.55±16.1*	365.11±33.8	370.89±44.3	523.14±17.0*	433.76±46.7	431.49±31.3
Stroke volume, μL	46.82±7.3	46.38±6.8	45.64±6.2	44.10±5.3	26.00±4.3*	30.78±4.5*	35.45±4.9*	27.37±7.6*	32.27±6.3*	38.33±6.6	59.17±7.0	30.78±3.4*	29.06±3.3*	30.10±6.7*	33.68±11.5*	38.87±5.9*	45.56±5.6

A 1-way ANOVA followed by Tukey's post hoc multiple comparisons test between groups was used to test for differences in main effect of treatment between groups. N, 4–7 mice per group. bpm indicates beats per minute; LPS, lipopolysaccharide; LVeDD, left ventricular end diastolic diameter; LVeSD, left ventricular end systolic diameter; rPHB1, recombinant human prohibitin 1; Veh, vehicle; and WT, wild type.
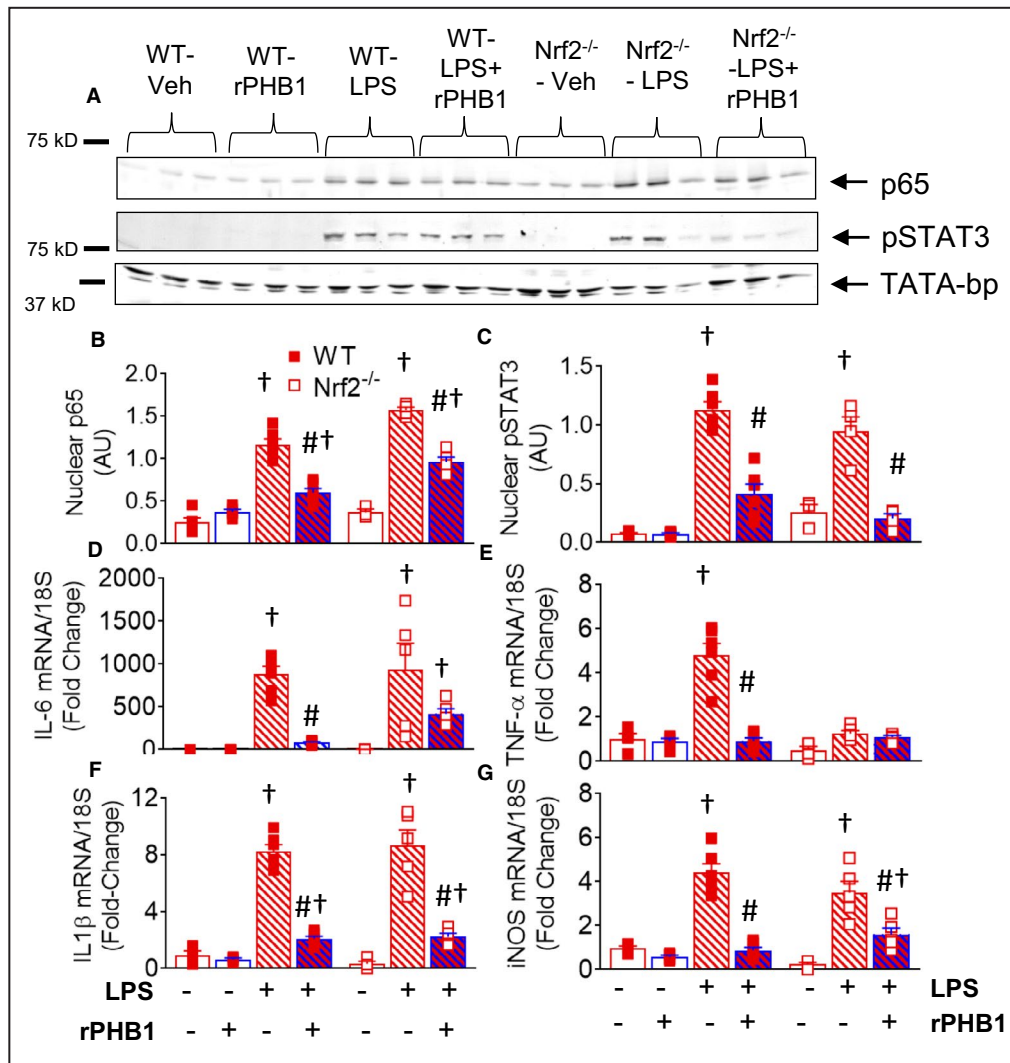*$P<0.05$ vs untreated mice (Vehicle), for that respective time point and genotype.

levels, but rPHB1 completely attenuated these markers (Figure S7).

Mitochondria produce ROS continuously in cardiomyocytes, necessitating a robust antioxidant network to maintain redox balance. During sepsis, mitochondrial ROS production increases because of many factors, including disruptions in oxidative phosphorylation, mitochondrial fission/mitophagy, and loss of antioxidant capacity.[9,46–48] In the present study, rPHB1 dosing, on its own, significantly diminished cardiac mitochondrial ROS production in WT, but not Nrf2−/− mice (Figure S8A). To determine the contribution of the mitochondrial redox enzyme thioredoxin reductase-2, we used the thioredoxin reductase inhibitor auranofin, a gold thiolate salt that we and others have used to elucidate the role of thioredoxin reductase-2 in the mitochondrial redox adaptations to exercise and cardiometabolic diseases.[38,49,50] Auranofin significantly increased mitochondrial ROS in all experimental groups. Interestingly, the auranofin-stimulated ROS was diminished with lipopolysaccharide challenge in both WT and Nrf2−/− mice, and substantially more so in the Nrf2−/− mice (Figure S8A). Conversely, rPHB1 dosing increased the auranofin-stimulated effect. This corresponded with increased rPHB1-induced expression of thioredoxin reductase-2 enzyme in WT, but not Nrf2−/− mice (Figure S8B). Treatment with rPHB1 also upregulated glutathione reductase enzyme in WT but not Nrf2−/− mice (Figure S8C).

The deleterious role of nitric oxide synthase in septic cardiomyopathy has been well-characterized.[51–53] To determine whether the rPHB1-mediated rescue of myocardial dysfunction in our model was associated with altered cardiac inducible nitric oxide synthase, we examined this enzyme in hearts of the mice used in this study. With rPHB1 dosing there was substantial downregulation of inducible nitric oxide synthase expression at both the mRNA and protein level in WT mice (Figure S9). No significant effect of rPHB1 dosing on inducible nitric oxide synthase was observed in Nrf2−/− mice, although these mice had diminished expression of inducible nitric oxide synthase at baseline compared with WT.

Cardioprotective Effects of rPHB1 Are Mediated in Part by PI3K/AKT Pathway Activation

Previous reports have linked PHB1 with coordination of intracellular signaling at plasma membrane lipid rafts via recruitment and activation (ie, phosphorylation) of serine/threonine kinase AKT, the master regulator of cell survival and metabolism.[20,54] We next examined whether the cardioprotective effect of rPHB1 acts via similar mechanism and found that rPHB1 caused

Figure 5. rPHB1 attenuates cardiac inflammation during endotoxemia independent of Nrf2.
Representative immunoblots of p65 (NFkB) and phospho-STAT3 from nuclear extracts prepared from WT and Nrf2$^{-/-}$ mouse hearts dissected 4 hours after LPS challenge and 2 hours after 1 dose of rPHB1 (300 ng) are shown in (**A**), and quantified via densitometry using the nuclear marker TATA-binding protein as loading control (**B, C**). Expression of pro-inflammatory cytokines IL6, TNFα, IL1β and iNOS (**D** through **G**) were also measured in whole heart tissue from this same cohort of mice. N=4–6 mice in each group. A 1-way ANOVA followed by Tukey's post hoc multiple comparisons test between groups was used to test for differences in main effect of LPS and rPHB1 treatment within each genotype. $^{†}P<0.05$ vs untreated mice (Baseline), for that respective time point and genotype; $^{#}P<0.05$ vs LPS alone, for that respective time point and genotype. IL1β indicates interleukin β; IL6, interleukin 6; i NOS, inducible nitric oxide synthase; LPS, lipopolysaccharide; Nrf2, nuclear factor (erythroid-derived 2)-like 2; rPHB1, recombinant human prohibitin 1; TNFα, tumor necrosis factor α; and WT, wild type.

a significant increase in AKT phosphorylation in human AC16 cardiomyocytes after 1 hour (Figure 6A). Importantly, this rPHB1-induced phosphorylation of AKT was not significantly affected by C-Raf inhibitor AZ628, but was completely abrogated by the PI3K inhibitor buparlisib, suggesting that rPHB1 activates AKT via PI3K-dependent mechanism (Figure 6A). To determine whether the protective effect of rPHB1 in the heart during endotoxemia was also dependent on PI3K/AKT pathway, WT mice were subjected to

lipopolysaccharide challenge (12 mg/kg) and rPHB1 dosing in absence and presence of buparlisib. PI3K inhibition in this model blunted the cardioprotective effect afforded by rPHB1 (Figure 6B). Immunoblot analysis showed that rPHB1 dosing caused an ≈3-fold upregulation of phospho-AKT levels in the hearts of these mice, which was attenuated with buparlisib (Figure 6C and 6D), consistent with what was observed in the AC16 cardiomyocytes. Interestingly, despite the severe cardiac dysfunction caused by buparlisib when
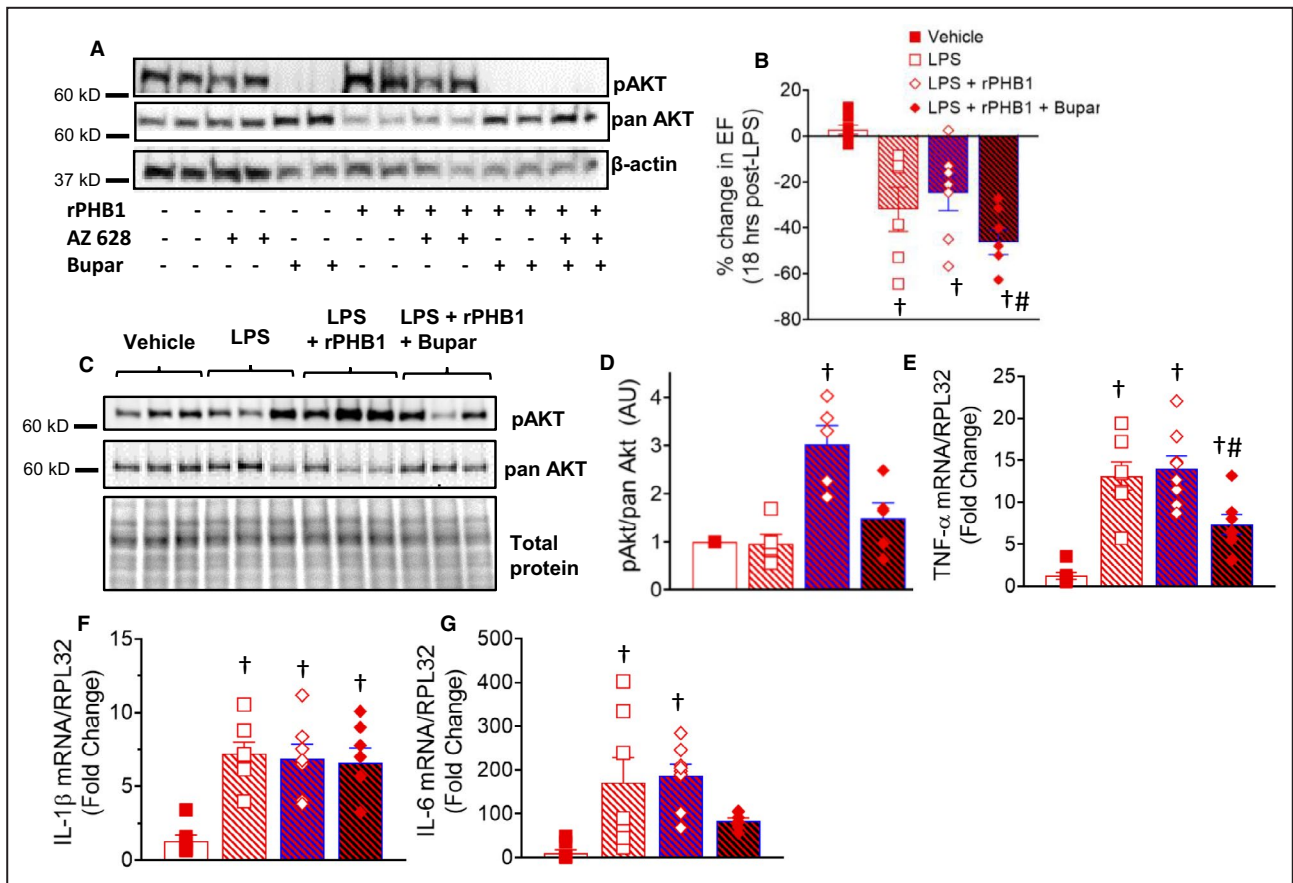
Figure 6. Protective effect of rPHB1 during endotoxemia is mediated by PI3K/AKT pathway in heart.
Effect of 1-hour treatment of rPHB1 (100 ng) on Akt phosphorylation in AC16 cardiomyocytes in absence and presence of the C-Raf inhibitor, AZ628, or PI3K inhibitor, buparlisib, is shown in (**A**). The effect of 3 doses of rPHB1 (300 ng) on cardiac systolic function in WT mice measured 18 hours after LPS challenge (12 mg/kg) in absence and presence of buparlisib is shown in (**B**), with levels of Akt phosphorylation in hearts dissected from this same cohort of mice (**C, D**). Expression of pro-inflammatory cytokines TNFα (**E**), IL1β (**F**) and IL-6 (**G**) were also measured in whole heart tissue. Cell culture immunoblots shown are representative of 2 independent experiments. For mouse models, N=5–7 mice in each group. A 1-way ANOVA followed by Tukey's post hoc multiple comparisons test between groups was used to test for differences in main effect of treatment between groups. [†]$P<0.05$ vs Vehicle-treated mice, [#]$P<0.05$ vs LPS + rPHB1. Bupar indicates buparlisib; IL1β, interleukin β; IL6, interleukin 6; LPS, lipopolysaccharide; rPHB1, recombinant human prohibitin 1; TNFα, tumor necrosis factor α; and WT, wild type.

combined with lipopolysaccharide + rPHB1, expression of pro-inflammatory cytokines TNFα and IL-6, but not IL-1β, were substantially lower with buparlisib (Figure 6E through 6G), suggesting that the cardioprotection afforded by rPHB1 is not exclusively because of its anti-inflammatory effect.

DISCUSSION

PHBs have pleiotropic roles in mammalian cells, and emerging evidence has implicated a role for these proteins in a wide variety of diseases including cancer, obesity/diabetes mellitus, and neurodegenerative and chronic inflammatory diseases.[55] Our findings have revealed a role for PHB1 in mitigating systemic inflammation and cardiac dysfunction during sepsis. These findings are important and distinct because we

demonstrate that (1) PHB1 is a highly dynamic protein that mobilizes within the cell and bloodstream during the acute phase response; (2) overexpression or administration of human rPHB1 preserves mitochondrial integrity and energetics in cardiomyocytes during inflammatory stress; (3) endogenous PHB1 behaves like an acute phase reactant in the bloodstream during endotoxemia and severe sepsis, and its secretion from hepatocytes is mediated by Nrf2; (4) dosing of human rPHB1 mitigates inflammation in vital organs during endotoxemia, and completely restores cardiac function, preserves cardiac mitochondrial energetics, and augments antioxidant capacity during endotoxemia independent of Nrf2; and (5) the cardioprotective effect of rPHB1 during endotoxemia is mediated, at least in part, by PI3K/AKT signaling. A schematic summarizing the overall findings of this study is shown in Figure 7.

These findings are translational and potentially of clinical importance as they suggest that PHB1 and its downstream signaling effectors are not only provocative drug targets, but PHB1 itself may, in certain contexts, be therapeutic.

Acute phase reactants have been defined as proteins whose concentration in the blood change from baseline (up or down) by >25% during an inflammatory response.[43,56] While it may be premature to call PHB1 a bona fide acute phase reactant at this point, it is clear that PHB1 fits these criteria as shown in Figure 1. The principal source of acute phase reactants during sepsis is the liver, and, while we have not definitively shown that liver is the only source of circulating PHB1, it is clear from Figure 3 that hepatocytes dramatically ramp up PHB1 expression and secretion in response

to lipopolysaccharide, and PHB1 secretion, but not expression, is regulated by Nrf2. Acute phase proteins have diverse actions in the host, ranging from coordination of both pro-inflammatory and anti-inflammatory responses, to recruitment of innate immune cells and regulation of vascular permeability and hemostasis. Some of these proteins possess both pro- and anti-inflammatory effects, depending on dose and time. An example of this is CRP (C-reactive protein), which is essential for coordinating clearance of foreign pathogens and activation of the complement system.[57,58] However, the overproduction of CRP in transgenic mice can also be anti-inflammatory and protective in models of septic shock.[59,60] This is thought to be due in large part to the inhibiting effect of CRP and its degradation products on neutrophil activation and
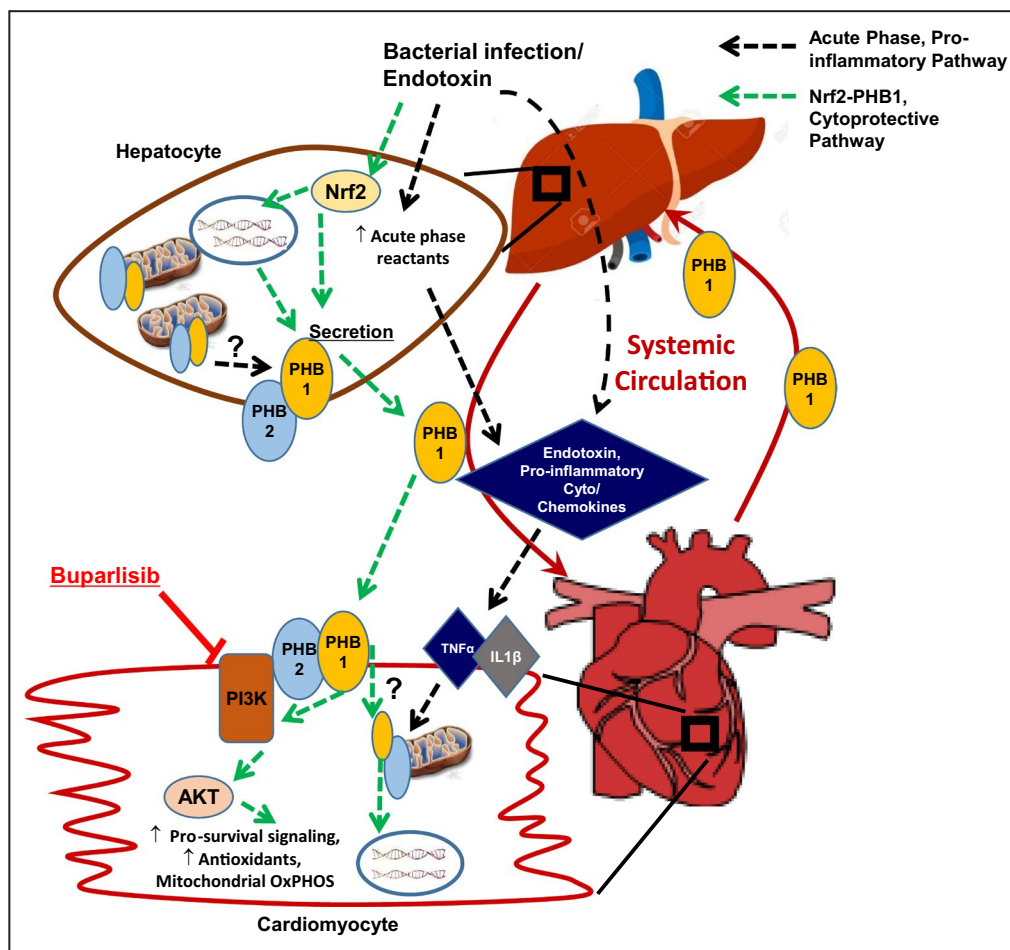

Figure 7.   Model of cardioprotective, anti-inflammatory effect of circulating PHB1 during sepsis.
A summary schematic of the overall findings uncovered in the present study are shown. Upon exposure to endotoxin, hepatocytes secrete pro-inflammatory acute phase reactant cyto/chemokines such as TNFα and IL1β. Our findings suggest that in parallel with this canonical pro-inflammatory response to endotoxin, Nrf2 mediates an anti-inflammatory response in hepatocytes via secretion of PHB1, either directly or indirectly via transcriptional activation of downstream target genes. As a circulating paracrine factor, PHB1 has systemic anti-inflammatory effects and acts directly on cardiomyocytes to upregulate pro-survival signaling and preserve mitochondrial OxPHOS independently of Nrf2, mediated in part via PI3K/AKT activation. IL1β indicates interleukin β; Nrf2, nuclear factor (erythroid-derived 2)-like 2; OxPHOS, oxidative phosphorylation; PHB1, prohibitin 1; and TNFα, tumor necrosis factor α.

extravasation.[61] Whether circulating PHB1 is having a similar effect on complement and neutrophils remains to be determined, since recent studies on PHBs in the innate immune system have focused solely on the intracellular signaling roles of these proteins, ignoring their role in the circulation.[62,63]

A link between PHBs and protection from oxidative/inflammatory stress has been well-documented in numerous cell types, including cardiomyocytes,[22,26–29] although a clear mechanism for how PHBs are functionally involved in this antioxidant/anti-inflammatory effect has not been fully elucidated. A detailed mechanism for how intracellular PHB1 inhibits TNFα-induced nuclear translocation of nuclear factor κ light-chain-enhancer of activated B cells was outlined in colonic epithelial cells by Theiss and colleagues, who demonstrated that PHB1 downregulates expression of importin α3, a protein required for nuclear factor κ light-chain-enhancer of activated B cells nuclear import.[42] Further work by this group outlined a role for PHB1 in protection against inflammatory bowel disease by upregulation of Nrf2 in colonic epithelium, corresponding to increased antioxidant gene expression.[29] However, in subsequent work, Nrf2 was found to be nonessential for the protective effect of PHB1, as there was a similar protective effect of PHB1 overexpression on colitis in Nrf2^{-/-} mice as in WT.[64] Our findings show that Nrf2 is essential for secretion of PHB1 from hepatocytes in endotoxemia (Figure 3), but Nrf2 is nonessential for the rescue of cardiac dysfunction and inflammation with human rPHB1 in endotoxemia (Figures 4 and 5). Much work remains to delineate the mechanisms by which PHB1 is regulated and secreted from cells during the acute phase, as it is clear that Nrf2 target gene(s) are likely involved.

A number of elegant studies have illustrated that PHBs are critical for optimal mitochondrial cristae organization and morphology, in part via regulation of cardiolipin and membrane fission-fusion. The latter process has been reported to be regulated by a partnership between PHBs and the dynamin-like GTPase, OPA1.[24,65–67] Following exposure to TNFα/IL-1β, mitochondrial PHB1 depletion (and nuclear accumulation) occurred simultaneously with mitochondrial fission, loss of ATP, production and decreased respiration in cardiomyocytes (Figures 1 and 2). One of our more surprising findings is that rPHB1 improved cardiac ATP production in endotoxemia (Figure 4G) while having no effect at all on improving the decrease in ADP-stimulated respiration following lipopolysaccharide challenge (Figure 4F and Figure S5). It is possible that rPHB1 is mitigating an inhibitory effect of inflammatory cyto/chemokines on enzymes in the phosphorylation system (eg, adenine nucleotide translocase, H+-ATPase), rather than components of the electron transport system or TCA cycle. Given the effect of rPHB1 alone on cardiac mitochondrial ROS, and that rPHB1 increases thioredoxin reductase-2 expression and auranofin-inhibitable ROS in the heart (Figure S8), it is plausible that some of the cardioprotective effects of rPHB1 are coming from enhanced mitochondrial antioxidant capacity. In any case, much more work is needed to identify the mechanisms by which cytokine-induced mitochondrial PHB1 depletion leads to impaired ATP production, and in turn, how recombinant PHB1 restores it.

Our preliminary findings implicate a role for PI3K/AKT pathway in mediating the paracrine-like protective effect of rPHB1 in the heart (Figure 6), though we cannot exclude the possibility that some uptake of rPHB1 into the cardiomyocytes is mediating this effect. In a pancreatic cell line, human rPHB1 treatment protected the cells from ethanol toxicity, and the authors provided evidence that cellular uptake of rPHB1 was responsible for the effect.[22] PHBs are on plasma membrane as well as mitochondrial membranes, and molecules from both bacterial[68] and synthetic origin[69] are capable of targeting cell surface PHB to facilitate cellular internalization. Though we were not able to comprehensively define the mechanisms by which rPHB1 protects the heart during endotoxemia, the fact that pro-inflammatory cytokine expression was actually blunted by buparlisib (Figure 6E through 6G) suggests that the protective effects of rPHB1 in heart are mediated by additional mechanisms unrelated to its anti-inflammatory effects.

Collectively, our findings suggest that PHB1 has an important role in the acute phase response to sepsis. Furthermore, we provide evidence that circulating PHB1 is anti-inflammatory and cardioprotective in a model of endotoxemia and severe sepsis, but only when administered at doses corresponding to 10-fold increase over physiological levels. This suggests that circulating PHB1 is only one part of a complex cascade of acute phase reactants that have inflammation-resolving effects. The protective effects of rPHB1 are complex and may be highly dependent on the tissue, underlying metabolic factors, and the time during progression of sepsis at which the effect is observed. Studies directed at establishing more detailed insight into how intracellular PHB1 mobilization and trafficking occurs, in addition to identifying interactors of PHB1 in the blood, are beyond the scope of the present study but will be necessary for therapeutic exploitation of these pathways to treat inflammatory disorders. The use of circulating PHB1 as a biomarker of organ dysfunction in patients with sepsis may also be of clinical significance, and these studies are ongoing.

ARTICLE INFORMATION

Affiliations

Department of Pharmacology & Toxicology, Brody School of Medicine, East Carolina University, Greenville, NC (T.A.M., C.P., J.R., B.K., K.M.G.); Medical Research Council Mitochondrial Biology Unit, University of Cambridge, United Kingdom (M.P.M.); Department of Pharmaceutical Sciences & Experimental Therapeutics, College of Pharmacy, Iowa City, IA (E.J.A.); and Fraternal Order of Eagles Diabetes Research Center, University of Iowa, Iowa City, IA (K.W., E.J.A.).

Acknowledgments

Sources of Funding

Disclosures

None.

Supplementary Material

Data S1
Table S1–S2
Figure S1–S9
References 38–41,70–77

REFERENCES

1. Antonucci E, Fiaccadori E, Donadello K, Taccone FS, Franchi F, Scolletta S. Myocardial depression in sepsis: from pathogenesis to clinical manifestations and treatment. *J Crit Care*. 2014;29:500–511. DOI: 10.1016/j.jcrc.2014.03.028.

2. Sanfilippo F, Corredor C, Fletcher N, Landesberg G, Benedetto U, Foex P, Cecconi M. Diastolic dysfunction and mortality in septic patients: a systematic review and meta-analysis. *Intensive Care Med*. 2015;41:1004–1013. DOI: 10.1007/s00134-015-3748-7.

3. Palmieri V, Innocenti F, Guzzo A, Guerrini E, Vignaroli D, Pini R. Left ventricular systolic longitudinal function as predictor of outcome in patients with sepsis. *Circ Cardiovasc Imaging*. 2015;8:e003865. DOI: 10.1161/CIRCIMAGING.115.003865.

4. Prucha M, Bellingan G, Zazula R. Sepsis biomarkers. *Clin Chim Acta*. 2015;440:97–103. DOI: 10.1016/j.cca.2014.11.012.

5. van Engelen TSR, Wiersinga WJ, Scicluna BP, van der Poll T. Biomarkers in sepsis. *Crit Care Clin*. 2018;34:139–152. DOI: 10.1016/j.ccc.2017.08.010.

6. Vincent JL, Bakker J, Marecaux G, Schandene L, Kahn RJ, Dupont E. Administration of anti-TNF antibody improves left ventricular function in septic shock patients. Results of a pilot study. *Chest*. 1992;101:810–815. DOI: 10.1378/chest.101.3.810.

7. Bujak M, Frangogiannis NG. The role of IL-1 in the pathogenesis of heart disease. *Arch Immunol Ther Exp (Warsz)*. 2009;57:165–176. DOI: 10.1007/s00005-009-0024-y.

8. Pathan N, Franklin JL, Eleftherohorinou H, Wright VJ, Hemingway CA, Waddell SJ, Griffiths M, Dennis JL, Relman DA, Harding SE, et al. Myocardial depressant effects of interleukin 6 in meningococcal sepsis are regulated by p38 mitogen-activated protein kinase. *Crit Care Med*. 2011;39:1692–1711. DOI: 10.1097/CCM.0b013e3182186d27.

9. Cimolai MC, Alvarez S, Bode C, Bugger H. Mitochondrial mechanisms in septic cardiomyopathy. *Int J Mol Sci*. 2015;16:17763–17778. DOI: 10.3390/ijms160817763.

10. Arulkumaran N, Deutschman CS, Pinsky MR, Zuckerbraun B, Schumacker PT, Gomez H, Gomez A, Murray P, Kellum JA, Workgroup AX. Mitochondrial function in sepsis. *Shock*. 2016;45:271–281. DOI: 10.1097/SHK.0000000000000463.

11. Alvarez S, Vico T, Vanasco V. Cardiac dysfunction, mitochondrial architecture, energy production, and inflammatory pathways: interrelated aspects in endotoxemia and sepsis. *Int J Biochem Cell Biol*. 2016;81:307–314. DOI: 10.1016/j.biocel.2016.07.032.

12. Kumar G, Kumar N, Taneja A, Kaleekal T, Tarima S, McGinley E, Jimenez E, Mohan A, Khan RA, Whittle J, et al. Nationwide trends of severe sepsis in the 21st century (2000–2007). *Chest*. 2011;140:1223–1231. DOI: 10.1378/chest.11-0352.

13. Lagu T, Rothberg MB, Shieh MS, Pekow PS, Steingrub JS, Lindenauer PK. Hospitalizations, costs, and outcomes of severe sepsis in the United States 2003 to 2007. *Crit Care Med*. 2012;40:754–761. DOI: 10.1097/CCM.0b013e318232db65.

14. Ande SR, Mishra S. Prohibitin interacts with phosphatidylinositol 3,4,5-triphosphate (PIP3) and modulates insulin signaling. *Biochem Biophys Res Commun*. 2009;390:1023–1028. DOI: 10.1016/j.bbrc.2009.10.101.

15. Ande SR, Nguyen KH, Padilla-Meier GP, Wahida W, Nyomba BL, Mishra S. Prohibitin overexpression in adipocytes induces mitochondrial biogenesis, leads to obesity development, and affects glucose homeostasis in a sex-specific manner. *Diabetes*. 2014;63:3734–3741. DOI: 10.2337/db13-1807.

16. Osman C, Haag M, Potting C, Rodenfels J, Dip PV, Wieland FT, Brugger B, Westermann B, Langer T. The genetic interactome of prohibitins: coordinated control of cardiolipin and phosphatidylethanolamine by conserved regulators in mitochondria. *J Cell Biol*. 2009;184:583–596. DOI: 10.1083/jcb.200810189.

17. Supale S, Thorel F, Merkwirth C, Gjinovci A, Herrera PL, Scorrano L, Meda P, Langer T, Maechler P. Loss of prohibitin induces mitochondrial damages altering beta-cell function and survival and is responsible for gradual diabetes development. *Diabetes*. 2013;62:3488–3499. DOI: 10.2337/db13-0152.

18. Wei Y, Chiang WC, Sumpter R Jr, Mishra P, Levine B. Prohibitin 2 is an inner mitochondrial membrane mitophagy receptor. *Cell*. 2017;168:224–238 e10. DOI: 10.1016/j.cell.2016.11.042.

19. Rajalingam K, Wunder C, Brinkmann V, Churin Y, Hekman M, Sievers C, Rapp UR, Rudel T. Prohibitin is required for Ras-induced Raf-MEK-ERK activation and epithelial cell migration. *Nat Cell Biol*. 2005;7:837–843. DOI: 10.1038/ncb1283.

20. Chiu CF, Ho MY, Peng JM, Hung SW, Lee WH, Liang CM, Liang SM. Raf activation by Ras and promotion of cellular metastasis require phosphorylation of prohibitin in the raft domain of the plasma membrane. *Oncogene*. 2013;32:777–787. DOI: 10.1038/onc.2012.86.

21. Martin B, Sanz R, Aragues R, Oliva B, Sierra A. Functional clustering of metastasis proteins describes plastic adaptation resources of breast-cancer cells to new microenvironments. *J Proteome Res*. 2008;7:3242–3253. DOI: 10.1021/pr800137w.

22. Lee JH, Nguyen KH, Mishra S, Nyomba BL. Prohibitin is expressed in pancreatic beta-cells and protects against oxidative and proapoptotic effects of ethanol. *FEBS J*. 2010;277:488–500. DOI: 10.1111/j.1742-4658.2009.07505.x.

23. Zhu B, Zhai J, Zhu H, Kyprianou N. Prohibitin regulates TGF-beta induced apoptosis as a downstream effector of Smad-dependent and -independent signaling. *Prostate*. 2010;70:17–26. DOI: 10.1002/pros.21033.

24. Merkwirth C, Dargazanli S, Tatsuta T, Geimer S, Lower B, Wunderlich FT, von Kleist-Retzow JC, Waisman A, Westermann B, Langer T. Prohibitins control cell proliferation and apoptosis by regulating OPA1-dependent cristae morphogenesis in mitochondria. *Genes Dev*. 2008;22:476–488. DOI: 10.1101/gad.460708.

25. Joshi B, Ko D, Ordonez-Ercan D, Chellappan SP. A putative coiled-coil domain of prohibitin is sufficient to repress E2F1-mediated transcription and induce apoptosis. *Biochem Biophys Res Commun*. 2003;312:459–466. DOI: 10.1016/j.bbrc.2003.10.148.

26. Muraguchi T, Kawawa A, Kubota S. Prohibitin protects against hypoxia-induced H9c2 cardiomyocyte cell death. *Biomed Res*. 2010;31:113–122. DOI: 10.2220/biomedres.31.113.

27. Liu X, Ren Z, Zhan R, Wang X, Wang X, Zhang Z, Leng X, Yang Z, Qian L. Prohibitin protects against oxidative stress-induced cell injury in cultured neonatal cardiomyocyte. *Cell Stress Chaperones*. 2009;14:311–319. DOI: 10.1007/s12192-008-0086-5.

28. Theiss AL, Idell RD, Srinivasan S, Klapproth JM, Jones DP, Merlin D, Sitaraman SV. Prohibitin protects against oxidative stress in intestinal epithelial cells. *FASEB J*. 2007;21:197–206. DOI: 10.1096/fj.06-6801com.

29. Theiss AL, Vijay-Kumar M, Obertone TS, Jones DP, Hansen JM, Gewirtz AT, Merlin D, Sitaraman SV. Prohibitin is a novel regulator of

antioxidant response that attenuates colonic inflammation in mice. *Gastroenterology*. 2009;137:199–208, 208 e1–6. DOI: 10.1053/j.gastro.2009.03.033.

30. Mishra S, Moulik S, Murphy LJ. Prohibitin binds to C3 and enhances complement activation. *Mol Immunol*. 2007;44:1897–1902. DOI: 10.1016/j.molimm.2006.09.025.

31. Mengwasser J, Piau A, Schlag P, Sleeman JP. Differential immunization identifies PHB1/PHB2 as blood-borne tumor antigens. *Oncogene*. 2004;23:7430–7435. DOI: 10.1038/sj.onc.1207987.

32. Mojtahedi Z, Safaei A, Yousefi Z, Ghaderi A. Immunoproteomics of HER2-positive and HER2-negative breast cancer patients with positive lymph nodes. *OMICS*. 2011;15:409–418. DOI: 10.1089/omi.2010.0131.

33. Ren H, Du N, Liu G, Hu HT, Tian W, Deng ZP, Shi JS. Analysis of variabilities of serum proteomic spectra in patients with gastric cancer before and after operation. *World J Gastroenterol*. 2006;12:2789–2792. DOI: 10.3748/wjg.v12.i17.2789.

34. Tompkins SC, Sheldon RD, Rauckhorst AJ, Noterman MF, Solst SR, Buchanan JL, Mapuskar KA, Pewa AD, Gray LR, Oonthonpan L, et al. Disrupting mitochondrial pyruvate uptake directs glutamine into the TCA cycle away from glutathione synthesis and impairs hepatocellular tumorigenesis. *Cell Rep*. 2019;28:2608–2619 e6. DOI: 10.1016/j.celrep.2019.07.098.

35. Gray L, Sultana M, Rauckhorst A, Oonthonpan L, Tompkins S, Sharma A, Fu X, Miao R, Pewa A, Brown K, et al. Hepatic mitochondrial pyruvate carrier 1 is required for efficient regulation of gluconeogenesis and whole-body glucose homeostasis. *Cell Metab*. 2015;22:669–681. DOI: 10.1016/j.cmet.2015.07.027.

36. Prescott MJ, Lidster K. Improving quality of science through better animal welfare: the NC3Rs strategy. *Lab Anim (NY)*. 2017;46:152–156. DOI: 10.1038/laban.1217.

37. Anderson EJ, Thayne K, Harris M, Carraway K, Shaikh SR. Aldehyde stress and up-regulation of Nrf2-mediated antioxidant systems accompany functional adaptations in cardiac mitochondria from mice fed n-3 polyunsaturated fatty acids. *Biochem J*. 2012;441:359–366. DOI: 10.1042/BJ20110626.

38. Fisher-Wellman KH, Mattox TA, Thayne K, Katunga LA, La Favor JD, Neufer PD, Hickner RC, Wingard CJ, Anderson EJ. Novel role for thioredoxin reductase-2 in mitochondrial redox adaptations to obesogenic diet and exercise in heart and skeletal muscle. *J Physiol*. 2013;591:3471–3486. DOI: 10.1113/jphysiol.2013.254193.

39. Lark DS, Torres MJ, Lin CT, Ryan TE, Anderson EJ, Neufer PD. Direct real-time quantification of mitochondrial oxidative phosphorylation efficiency in permeabilized skeletal muscle myofibers. *Am J Physiol Cell Physiol*. 2016;311:C239–C245. DOI: 10.1152/ajpcell.00124.2016.

40. Anderson EJ, Rodriguez E, Anderson CA, Thayne K, Chitwood WR, Kypson AP. Increased propensity for cell death in diabetic human heart is mediated by mitochondrial-dependent pathways. *Am J Physiol Heart Circ Physiol*. 2011;300:H118–H124. DOI: 10.1152/ajpheart.00932.2010.

41. Boyle KE, Zheng D, Anderson EJ, Neufer PD, Houmard JA. Mitochondrial lipid oxidation is impaired in cultured myotubes from obese humans. *Int J Obes (Lond)*. 2012;36:1025–1031. DOI: 10.1038/ijo.2011.201.

42. Theiss AL, Jenkins AK, Okoro NI, Klapproth JM, Merlin D, Sitaraman SV. Prohibitin inhibits tumor necrosis factor alpha-induced nuclear factor-kappa B nuclear translocation via the novel mechanism of decreasing importin alpha3 expression. *Mol Biol Cell*. 2009;20:4412–4423. DOI: 10.1091/mbc.e09-05-0361.

43. Gabay C, Kushner I. Acute-phase proteins and other systemic responses to inflammation. *N Engl J Med*. 1999;340:448–454. DOI: 10.1056/NEJM199902113400607.

44. Vary TC, Kimball SR. Regulation of hepatic protein synthesis in chronic inflammation and sepsis. *Am J Physiol*. 1992;262:C445–C452. DOI: 10.1152/ajpcell.1992.262.2.C445.

45. Thimmulappa RK, Lee H, Rangasamy T, Reddy SP, Yamamoto M, Kensler TW, Biswal S. Nrf2 is a critical regulator of the innate immune response and survival during experimental sepsis. *J Clin Invest*. 2006;116:984–995. DOI: 10.1172/JCI25790.

46. Suliman HB, Welty-Wolf KE, Carraway M, Tatro L, Piantadosi CA. Lipopolysaccharide induces oxidative cardiac mitochondrial damage and biogenesis. *Cardiovasc Res*. 2004;64:279–288. DOI: 10.1016/j.cardiores.2004.07.005.

47. Turner A, Tsamitros M, Bellomo R. Myocardial cell injury in septic shock. *Crit Care Med*. 1999;27:1775–1780. DOI: 10.1097/00003246-199909000-00012.

48. Gonzalez AS, Elguero ME, Finocchietto P, Holod S, Romorini L, Miriuka SG, Peralta JG, Poderoso JJ, Carreras MC. Abnormal mitochondrial fusion-fission balance contributes to the progression of experimental sepsis. *Free Radic Res*. 2014;48:769–783. DOI: 10.3109/10715762.2014.906592.

49. Aon MA, Stanley BA, Sivakumaran V, Kembro JM, O'Rourke B, Paolocci N, Cortassa S. Glutathione/thioredoxin systems modulate mitochondrial H2O2 emission: an experimental-computational study. *J Gen Physiol*. 2012;139:479–491. DOI: 10.1085/jgp.201210772.

50. Stanley BA, Sivakumaran V, Shi S, McDonald I, Lloyd D, Watson WH, Aon MA, Paolocci N. Thioredoxin reductase-2 is essential for keeping low levels of H(2)O(2) emission from isolated heart mitochondria. *J Biol Chem*. 2011;286:33669–33677. DOI: 10.1074/jbc.M111.284612.

51. Barth E, Radermacher P, Thiemermann C, Weber S, Georgieff M, Albuszies G. Role of inducible nitric oxide synthase in the reduced responsiveness of the myocardium to catecholamines in a hyperdynamic, murine model of septic shock. *Crit Care Med*. 2006;34:307–313. DOI: 10.1097/01.CCM.0000199070.46812.21.

52. Boyle WA III, Parvathaneni LS, Bourlier V, Sauter C, Laubach VE, Cobb JP. iNOS gene expression modulates microvascular responsiveness in endotoxin-challenged mice. *Circ Res*. 2000;87:E18–E24. DOI: 10.1161/01.RES.87.7.e18.

53. Xu C, Yi C, Wang H, Bruce IC, Xia Q. Mitochondrial nitric oxide synthase participates in septic shock myocardial depression by nitric oxide overproduction and mitochondrial permeability transition pore opening. *Shock*. 2012;37:110–115. DOI: 10.1097/SHK.0b013e3182391831.

54. Wu Q, Wu S. The role of lipid raft translocation of prohibitin in regulation of Akt and Raf-protected apoptosis of HaCaT cells upon ultraviolet B irradiation. *Mol Carcinog*. 2017;56:1789–1797. DOI: 10.1002/mc.22636.

55. Thuaud F, Ribeiro N, Nebigil CG, Desaubry L. Prohibitin ligands in cell death and survival: mode of action and therapeutic potential. *Chem Biol*. 2013;20:316–331. DOI: 10.1016/j.chembiol.2013.02.006.

56. Morley JJ, Kushner I. Serum C-reactive protein levels in disease. *Ann N Y Acad Sci*. 1982;389:406–418. DOI: 10.1111/j.1749-6632.1982.tb22153.x.

57. Ballou SP, Lozanski G. Induction of inflammatory cytokine release from cultured human monocytes by C-reactive protein. *Cytokine*. 1992;4:361–368. DOI: 10.1016/1043-4666(92)90079-7.

58. Cermak J, Key NS, Bach RR, Balla J, Jacob HS, Vercellotti GM. C-reactive protein induces human peripheral blood monocytes to synthesize tissue factor. *Blood*. 1993;82:513–520. DOI: 10.1182/blood.V82.2.513.513.

59. Xia D, Samols D. Transgenic mice expressing rabbit C-reactive protein are resistant to endotoxemia. *Proc Natl Acad Sci USA*. 1997;94:2575–2580. DOI: 10.1073/pnas.94.6.2575.

60. Ahmed N, Thorley R, Xia D, Samols D, Webster RO. Transgenic mice expressing rabbit C-reactive protein exhibit diminished chemotactic factor-induced alveolitis. *Am J Respir Crit Care Med*. 1996;153:1141–1147. DOI: 10.1164/ajrccm.153.3.8630558.

61. Heuertz RM, Ahmed N, Webster RO. Peptides derived from C-reactive protein inhibit neutrophil alveolitis. *J Immunol*. 1996;156:3412–3417.

62. Kim DK, Kim HS, Kim AR, Jang GH, Kim HW, Park YH, Kim B, Park YM, Beaven MA, Kim YM, et al. The scaffold protein prohibitin is required for antigen-stimulated signaling in mast cells. *Sci Signal*. 2013;6:ra80. DOI: 10.1126/scisignal.2004098.

63. Lucas CR, Cordero-Nieves HM, Erbe RS, McAlees JW, Bhatia S, Hodes RJ, Campbell KS, Sanders VM. Prohibitins and the cytoplasmic domain of CD86 cooperate to mediate CD86 signaling in B lymphocytes. *J Immunol*. 2013;190:723–736. DOI: 10.4049/jimmunol.1201646.

64. Kathiria AS, Butcher MA, Hansen JM, Theiss AL. Nrf2 is not required for epithelial prohibitin-dependent attenuation of experimental colitis. *Am J Physiol Gastrointest Liver Physiol*. 2013;304:G885–G896. DOI: 10.1152/ajpgi.00327.2012.

65. Merkwirth C, Martinelli P, Korwitz A, Morbin M, Bronneke HS, Jordan SD, Rugarli EI, Langer T. Loss of prohibitin membrane scaffolds impairs mitochondrial architecture and leads to tau hyperphosphorylation and neurodegeneration. *PLoS Genet*. 2012;8:e1003021. DOI: 10.1371/journal.pgen.1003021.

66. Tatsuta T, Model K, Langer T. Formation of membrane-bound ring complexes by prohibitins in mitochondria. *Mol Biol Cell*. 2005;16:248–259. DOI: 10.1091/mbc.e04-09-0807.

67. Richter-Dennerlein R, Korwitz A, Haag M, Tatsuta T, Dargazanli S, Baker M, Decker T, Lamkemeyer T, Rugarli EI, Langer T. DNAJC19, a mitochondrial cochaperone associated with cardiomyopathy, forms a complex with prohibitins to regulate cardiolipin remodeling. *Cell Metab*. 2014;20:158–171. DOI: 10.1016/j.cmet.2014.04.016.

68. Sharma A, Qadri A. Vi polysaccharide of Salmonella typhi targets the prohibitin family of molecules in intestinal epithelial cells and suppresses early inflammatory responses. *Proc Natl Acad Sci USA*. 2004;101:17492–17497. DOI: 10.1073/pnas.0407536101.

69. Kim DH, Woods SC, Seeley RJ. Peptide designed to elicit apoptosis in adipose tissue endothelium reduces food intake and body weight. *Diabetes*. 2010;59:907–915. DOI: 10.2337/db09-1141.

70. Saks VA, Veksler VI, Kuznetsov AV, Kay L, Sikk P, Tiivel T, Tranqui L, Olivares J, Winkler K, Wiedemann F, et al. Permeabilized cell and skinned fiber techniques in studies of mitochondrial function in vivo. *Mol Cell Biochem*. 1998;184:81–100.

71. Anderson EJ, Neufer PD. Type II skeletal myofibers possess unique properties that potentiate mitochondrial H(2)O(2) generation. *Am J Physiol Cell Physiol*. 2006;290:C844–C851.

72. Perry CG, Kane DA, Lin CT, Kozy R, Cathey BL, Lark DS, Kane CL, Brophy PM, Gavin TP, Anderson EJ, et al. Inhibiting myosin-ATPase reveals a dynamic range of mitochondrial respiratory control in skeletal muscle. *Biochem J*. 2011;437:215–222. DOI: 10.1042/BJ20110366.

73. Claycomb WC, Lanson NA Jr, Stallworth BS, Egeland DB, Delcarpio JB, Bahinski A, Izzo NJ Jr. HL-1 cells: a cardiac muscle cell line that contracts and retains phenotypic characteristics of the adult cardiomyocyte. *Proc Natl Acad Sci USA*. 1998;95:2979–2984. DOI: 10.1073/pnas.95.6.2979.

74. White SM, Claycomb WC. Cardiac cell transplantation: protocols and applications. *Methods Mol Biol*. 2003;219:83–95. DOI: 10.1385/1-59259-350-x:83.

75. White SM, Constantin PE, Claycomb WC. Cardiac physiology at the cellular level: use of cultured HL-1 cardiomyocytes for studies of cardiac muscle cell structure and function. *Am J Physiol Heart Circ Physiol*. 2004;286:H823–H829. DOI: 10.1152/ajpheart.00986.2003.

76. Deryckere F, Gannon F. A one-hour minipreparation technique for extraction of DNA-binding proteins from animal tissues. *Biotechniques*. 1994;16:405.

77. Tsien RY. Fluorescence measurement and photochemical manipulation of cytosolic free calcium. *Trends Neurosci*. 1988;11:419–424. DOI: 10.1016/0166-2236(88)90192-0.

SUPPLEMENTAL MATERIAL

Data S1.

Supplemental Materials and Methods

Preparation of permeabilized cardiac myofibers

This technique has been described by our group [70] and others [71] in detail. Following exsanguination the heart was removed, briefly rinsed in saline to remove excess blood, and a portion of the left ventricle (LV) near the apex was removed for mitochondrial experiments. LV samples were then placed in ice-cold (4∘C) Buffer X containing (mM): 7.23 K2EGTA, 2.77 CaK2EGTA, 20 imidazole, 20 taurine, 5.7 ATP, 14.3 phosphocreatine, 6.56 MgCl2.6H2O and 50Mes (pH 7.1, 295 mosmol l−1). Fat and connective tissue were removed from muscle samples under a dissecting microscope and small bundles of fibers were prepared (>1mg wet weight per fibers bundle). Fiber bundles were treated with 50 μg ml^{-1} saponin for 30 min as previously described.[72] Following permeabilization, myofiber bundles were washed in ice-cold Buffer Z containing (mM): 110 K-Mes, 35 KCl, 1 EGTA, 5 K2HPO2, 3 MgCl2.6H2O and 5mgml−1 bovine serum albumin (BSA; pH 7.4, 295 mosmol l−1) and remained in Buffer Z on a rotator at 4∘C until analysis (<4 h). We have observed that permeabilized myofibers bundles exhibit a very strong Ca2+-independent contraction that is temperature sensitive and can occur even at 4∘C;[72] therefore, 20 μM blebbistatin was added to the wash buffer, in addition to the respiration medium during experiments, to prevent contraction as previously described. Following permeabilization and washing in Buffer Z, all mitochondrial function measurements were completed in <4 hours.

HL-1 cardiomyocyte cell culture experiments

HL-1 cardiomyocytes are an immortalized cardiomyocyte cell line originally derived from mouse atrial cardiomyocytes [74-76], a kind gift from Dr. WC Claycomb (Louisiana State University Medical Centre, LA). Cells were cultured in Claycomb media (Sigma-Aldrich, St. Louis, MO) supplemented with 10% fetal bovine serum, 4mM L-glutamine, 10μM norepinephrine and MycoZap™Plus-CL (Lonza, Walkersville, MD) and maintained at 37°C and 5% CO_2. Experiments were performed on these cells prior to passage 20. In all experiments where TNFα and IL1β were used in these cells, the concentration was 3 and 100 (ng/mL) respectively (0.17nM TNFα and 5.71nM IL1β). These dosages were determined using a modified dose-response curve (**Figure S2**), where this dosage, when compared to control, showed an increase in nuclear localization of NFκB subunit p65. For recombinant PHB1 (rPHB1) exposure, cells were incubated with recombinant flag-tagged PHB (6.25uM or 200ng/mL) or transfected with a pCMV6-AC-GFP vector (Origene, Rocksville, MD) containing a human clone of PHB1 or a GFP positive scrambled vector. For over-expression of PHB1, we used a *PrecisionShuttle™ Vector System* (Origene, Rockville, MD) with a pCMV6-AV vector, which is a mammalian expression vector, containing the human PHB1 gene encoded in-frame with a green fluorescent protein (GFP) sequence on the C-terminal end. Transfection was performed at 75-80% of cell confluency. For the antioxidant response element (ARE) reporter assay, we used a *Lenti*

ARE reporter (GFP) System (Qiagen, Inc., Valencia, CA, USA) which is a preparation of VSV-g pseudotype lentivirus particles with minimal CMV promoter and tandem repeats of the ARE transcriptional response element controlling the expression of GFP.

Primary hepatocyte isolation

Livers were first perfused with a physiologically-neutral buffered solution containing collagenase and trypsin inhibitor. Using forceps and gentle agitation, hepatocytes were liberated from the liver capsule, and the initial cell suspension was centrifuged at 50 x *g* for 6 min. The supernatant, enriched with Kupffer, fibroblasts and other non-hepatocyte (non-parenchymal) cell types was then discarded, and the hepatocyte-enriched pellet was washed by gentle resuspension in a 5-ml pipet, followed by centrifugation for 3 minutes at 50 x *g* to further remove debris, dead cells, and non-parenchymal cells. This washing step was repeated twice. Hepatocytes were plated at a density of ~150,000 cells/cm^2 and allowed to attach for 4 hours in Williams E media, supplemented with 5% FBS, 1% Penicillin-Streptomycin, 10 nM insulin, and 10 nM dexamethasone.

Preparation of HL-1 cardiomyocytes for mitochondrial function assays.

Cells were lifted from culture flasks with 0.05% Trypsin-EDTA and counted using the Vi-Cell SGL (Beckman Coulter). The protocol for permeabilization was adapted from our previous work [70]. Briefly, 2.0 million cells (for mitochondrial O_2 consumption) and 1.0 million cells (for mitochondrial H_2O_2 and Ca^{2+} uptake) cells were centrifuged at 500xg for 5 minutes at room temperature. Cells used for mitochondrial O_2 consumption were resuspended in room temperature MiRO5 respiration buffer (110mM Sucrose, 60mM K-MES, 20mM HEPES, 20mM Taurine, 10mM KH_2PO_4, 3mM $MgCl_2·6H_2O$, 1mM EGTA and 2.5g/L BSA [pH=7.4 with KOH]) while cells for mitochondrial H_2O_2 and Ca^{2+} uptake were resuspended in room temperature buffer Z-lite (150mM K-MES, 30mM KCL, 10mM KH_2PO_4, 5mM $MgCl_2·6H_2O$, 1mM EGTA and 0.5mg/L BSA [pH=7.4]). Cells were permeabilized using 3.0 µg/million cells of digitonin (Sigma-Aldrich, St. Louis, MO) in final resuspension before functional assessment.

Subcellular Fractionation

Nuclear extracts were performed using fresh portions of cardiac tissue immediately after dissection and cardiomyocytes lifted using 0.05% trypsin/EDTA, according to the method described by Deryckere [78]. Briefly, after removal of connective tissue, the fresh myocardial tissue was placed in ice-cold hypotonic buffer (10 mM HEPES, pH 7.5; 40 mM NaF; 10 µM Na_2MoO_4; 0.1 mM EDTA, 1 mM β-glycerophosphate; 1 mM Na_3VO_4, and protease inhibitor cocktail (Sigma-Aldrich, St Louis, MO) and transferred to the laboratory. Tissue was then minced very fine, placed back into ice-cold hypotonic buffer, pulverized in a dounce homogenizer for 10-12 strokes, and incubated on ice for 15 minutes. The sample was then centrifuged at 300xg for 10 minutes and supernatant retained as a cytosolic fraction. Pellet was then resuspended in ice-cold hypotonic buffer and again incubated for 15 minutes on ice. Nonidet P-40 was added at 0.1X the sample volume and centrifuged at 14,000Xg for 30 seconds. This supernatant was also retained as the

cytosolic fraction, and pellet was resuspended in nuclear extraction buffer (10 mM HEPES, pH 7.9; 0.1 mM EDTA; 3 mM $MgCl_2$; 420 mM $NaCl_2$; 10% glycerol (v/v)), vortexed at full speed for 30 seconds and then incubated for 15 minutes at 4°C with rocking. This step was repeated. The sample was then centrifuged at 14,000Xg for 10 minutes at 4°C, and the supernatant retained as the nuclear fraction.

Mitochondrial O_2 consumption, ATP production, H_2O_2 emission, and Ca^{2+} uptake

All mitochondrial experiments in permeabilized cardiac myofibers and HL-1 cardiomyocytes were performed at 30°C. Buffer Z was used for permeabilized myofibers, while MiRO5 was used for permeabilized HL-1 cardiomyocytes. Mitochondrial O_2 consumption (J-O_2) was measured using the O_2K Oxygraph system (Oroboros Instruments, Austria) in buffer containing 20mM creatine monohydrate (Sigma-Aldrich, St. Louis, MO). Substrates and respiratory inhibitors were provided as indicated in the Figure legends. Simultaneous measurements of mitochondrial ATP production (J-ATP) were obtained using a custom tandem oxi-fluorometer approach developed and validated in our laboratory [79], by coupling ATP hydrolysis to NADPH production and auto-fluorescence. To maintain coupling of ATP hydrolysis to NADPH release, 2.5 U/mL of glucose-6-phosphate dehydrogenase (Roche, Indianapolis IN) 2.5 U/mL yeast hexokinase (Roche, Indianapolis IN), 5mM nicotinamide adenine dinucleotide phosphate (NADP+) (Sigma-Aldrich, St. Louis, MO), and 5mM D-glucose (Sigma-Aldrich, St. Louis, MO) were added to the assay media. P1,P5-Di(Adenosine-5′)Pentaphosphate (Ap5A) (Sigma-Aldrich, St. Louis, MO) was added to inhibit adenylate kinase and ensure that ATP production being measured by the system was solely from the mitochondria. Mitochondrial H_2O_2 and Ca^{2+} uptake measurements were conducted in a spectrofluorometer (Photon Technology Instruments, Birmingham, NJ). Mitochondrial H_2O_2 studies were performed in the presence of 125 µM ADP, 5mM glucose and 1 unit/ml hexokinase to keep the mitochondria in a permanent submaximal phosphorylating state. For mitochondrial H_2O_2 measurements, buffer Z-lite contained 10 µM Amplex Red, 3 unit/ml horseradish peroxidase, 25 units/mL superoxide dismutase (SOD), 5 mM pyruvate, 2 mM malate and 5 mM succinate, and the H_2O_2 emission rate was calculated as outlined previously. For Ca^{2+} uptake measurements, buffer Z-lite contained 1 µM Calcium Green 5-N, 5 mM pyruvate, 2 mM malate, 5 mM succinate. At the start of the Ca^{2+} uptake studies 1.5 µM thapsigargin was added to inhibit the sarcoplasmic/endoplasmic reticulum Ca^{2+}-ATPase (SERCA) and 10 µM EGTA, to chelate any remaining Ca^{2+}. Pulses of 30µmol Ca^{2+} ($CaCl_2$) were added sequentially and Ca^{2+} uptake was followed until the mitochondrial permeability transition pore opening, as described previously [80]. At the conclusion of the experiment, a 1 mM bolus of $CaCl_2$ was added to saturate the probe. Using the known Kd for Calcium Green 5-N and the F_{min} and F_{max} established during each experiment, changes in free calcium were calculated using the equations described by Tsien [81].

Real-time quantitative PCR

For mRNA extraction, cardiac samples frozen in liquid N_2 and HL1c were homogenized using a Pro Scientific Pro200 tissue homogenizer in 600µL and 350µL, respectively, and then subjected to a brief proteinase K treatment (55°C for 10 min). Total

mRNA was then extracted in RNeasy columns according to the manufacturer's instructions (Qiagen, Inc., Valencia, CA, USA). Reverse transcription and relative changes in mRNA of all redox- and anti-inflammatory target genes were determined by fluorescence-based real-time PCR using SsoAdvanced SYBR Green Supermix (BioRad Laboratories, Hercules, CA, USA). The primer pairs used in these experiments are listed in **Table S1**. Data were analyzed by the ΔΔCt (threshold cycle) method using Bio-Rad CFX Manager software and mRNA levels were normalized to β-Actin and 18S as appropriate.

Myocardial protein extraction and immunoblot

For whole tissue protein extracts, myocardial samples frozen in liquid N_2 were homogenized in ice-cold 10x (w/v) of TEE Buffer (10mM Tris-base; 1mM EDTA and 1mM EGTA pH 7.4) containing 0.5% Triton X-100 and protease inhibitor cocktail (Sigma-Aldrich, St. Louis, MO), using a glass grinder (Kimble Chase, Vineland, NJ). After 5 minute incubation on ice, homogenates were spun at 10,000 rpm for 10 minutes to pellet debris, and supernatants were retained for protein analysis. Proteins were separated based on molecular weight using SDS-PAGE. Following electrophoresis, proteins were transferred to Immobilon FL PVDF (Milipore, Billerica, MA) membrane using a semi-dry blot apparatus (Trans-Blot SD; Bio-Rad Laboratories, Hercules, CA). After transfer, membranes were blocked using 5% non-fat dry milk in tris-buffered saline with 0.1% Tween-20 (TBS-T) for at least 1 hour at room temperature, to prevent nonspecific antibody binding. Membranes were washed with TBS-T three times for 10 minutes and incubated overnight at 4°C with primary antibodies (see list in **Table S2**). The following day, membranes were washed with TBS-T three times for 15 minutes to remove any unbound primary antibody. Following washing, membranes were incubated with secondary antibodies for 1 hour at room temperature. Before imaging, membranes were washed three times for 10 minutes. Protein-antibody complexes were imaged using Odyssey® CLx (Li-Cor; Lincoln, NE). Densitometric analysis was performed using ImageJ software (National Institutes of Health).

Enzyme-linked immunosorbent assay (ELISA) of serum PHB1

Blood was drawn from the tail vein of the rats at baseline (time 0), and 4 and 12 hours following the induction of sepsis with LPS. At the 24 hour time point, blood was collected by cardiac puncture. In the mouse studies, blood was collected at 4 and 16 hours by cardiac puncture. The blood was centrifuged at 500xg for 5 minutes to separate the serum. Serum was removed and flash frozen in liquid nitrogen and stored at -80°C until the time of analysis. The absolute amount PHB1 in circulation determined by a quantitative ELISA approach developed in our lab. A standard curve of PHB1 was first established using purified recombinant PHB1 (Origene, Rockville, MD). Standards and diluted (1/5) serum samples were added to an Immunolon-coated 96-well assay plate (Fisher Scientific). Samples were incubated overnight at 4°C, and subsequently washed with PBS+0.05% Tween-20 and blocked for 2 hours with with 10% fetal bovine serum (Sigma-Aldrich, St. Louis, MO) diluted in PBS. Samples were then incubated with anti-PHB antibody (1:200 in PBS+0.05% BSA, Abcam) for 2 hours at 37°C. Samples were washed with PBS+0.05% Tween-20 and incubated with secondary antibody for 2 hours

at room temperature (goat anti-rabbit HRP, Bio-Rad). Following this incubation, samples were washed as before and incubated with 10 µM Amplex Red for 20 minutes at room temperature. Fluorescence values were then recorded with the 530ex/590em filter using a Synergy™ plate reader (BioTek Instruments, Winoski, VT). Total quantities of serum PHB in each group was determined using standard curve of rPHB, and expressed in absolute amount as ng/mL.

Immunocytochemistry

HL-1 cardiomyocytes were grown in glass bottom 6-well plates (MatTek Corporation). Where appropriate, 50nM MitoTracker® Red CMXRos was incubated on the cells for 15 minutes at 37°C after which the cells were washed twice in sterile PBS. Using 3.7% para-formaldehyde, cells were fixed. Fixative was washed off with PBS. Cells were permeabilized using 0.1% Triton X-100 and blocked using 5% goat serum. Cells were incubated with primary antibodies as indicated throughout (antibody information can be found in Table 2.3) overnight at 4°C. Cells were washed and incubated with secondary antibodies as indicated throughout (see Table 2.3 for antibody information) for 1 hour at room temperature. Cell were washed with PBS and incubated with Draq5 (Cell Signaling Technology, Danvers, MA) for 5 minutes. Cell microscopy was carried out with a Carl Zeiss LSM 510 using a 63X magnification.

Measurements of mitochondrial ROS production using MitoSox™Red were carried out in live cells. Cells were exposed to a cocktail of 3/100 (ng/mL) TNFα/IL1β for 24 hours. Following treatment the cells were incubated with 2 µM MitoSox™Red in buffer containing Ca and Mg for 10 minutes. Cell were then washed with PBS and imaged with a Nikon Eclipse Ti microscope using 20X magnification

Measurements of ARE-driven GFP fluorescence were carried out in live cells. Transfected cells were exposed to PBS as a vehicle control, 20 uM sulforophane (Sigma-Aldrich, St. Louis, MO), a cocktail of 3/100 (ng/mL) TNFα/IL1β only, rPHB1 (200ng/mL) only or a combination of rPHB1 and TNFα/IL1β (both applied at time 0 and rPHB1 added 12 hours after TNFα/IL1β) for 24 hours. Following treatment cells were washed with PBS and imaged using with a Nikon Eclipse Ti microscope using 20X magnification.

Cytotoxicity

Cell death was assessed 24 hours after the inflammatory insult using a commercially available lactate dehydrogenase (LDH) assay kit (Abcam, Cambridge, MA). Briefly, HL-1 cardiomyocytes were grown to 85% confluency in normal growth media. Upon reaching 85% confluency, cells were incubated in phenol-red free Opti-MEM media and treated with 3.0 ng/mL TNFα and 100 ng/mL IL1β. Following treatment, 100 µL of medium was removed to an optically clear 96-well plate. LDH Reaction Mix was added to each well and color development was monitored for 20-30 minutes. Absorbance was measured at 450 nm.

Table S1. Primers used for qRT-PCR.

Primers	Sequence (5'→3')
Prohibitin-1 Mouse	
Forward	GCATTGGCGAGGACTATGAT
Reverse	CTCTGTGAGGTCATCGCTCA
Nrf2 Mouse	
Forward	CTACTCGTGTGGGACAGCAA
Reverse	AGCAGACTCCAGGTCTTCCA
TNFα Mouse	
Forward	GTCCCCAAAGGGATGAGAAGT
Reverse	CAGCCACTCCAGCTGCTC
IL1β Mouse	
Forward	TGCCACCTTTTGACAGTGATG
Reverse	TGCCACCTTTTGACAGTGATG
IL6 Mouse	
Forward	GCCTTCTTGGGACTGATGCT
Reverse	TGCCATTGCACAACTCTTTTC
iNOS Mouse	
Forward	CCCTTCCGAAGTTTCTGGCAGCAGC
Reverse	CCCTTCCGAAGTTTCTGGCAGCAGC
COX2 Mouse	
Forward	CACTACATCCTGACCCACTT
Reverse	ATGCTCCTGCTTGAGTATGT
CRP Mouse	
Forward	AGCCTCTCTCATGCTTTTGG
Reverse	TGTCTCTTGGTGGCATACGA

NRF1 Mouse

Forward	TGGAGGAGCACGGAGTGA
Reverse	CAGCCAGATGGGCAGTTA

Rpl32 Mouse

Forward	AATTAAGCGAAACTGGCGGA
Reverse	GATCTGGCCCTTGAACCTTCTC

Tfam Mouse

Forward	CATTTATGTATCTGAAAGCTTCC
Reverse	CTCTTCCCAAGACTTCATTTC

Gpx1 Mouse

Forward	CTCACCCGCTCTTTACCTTCCT
Reverse	ACACCGGAGACCAAATGATGTACT

Gpx4 Mouse

Forward	TGAGGCAAAACTGACGTAAACTACA
Reverse	GCTCCTGCCTCCCAAACTG

Trx2 Mouse

Forward	CAGCCTCTGGCACATTTCCT
Reverse	GTTCGGCTTCTGGTTTCCTTT

NQO1 Mouse

Forward	CCATTCTGAAAGGCTGGTTTG
Reverse	CTAGCTTTGATCTGGTTGTC

HO1 Mouse

Forward	GCCTTGAAGGAGGCCACCAA
Reverse	CCTCAAACAGCTCAATGTTG

GCLC Mouse

Forward	GGAGGCTACTTCTGTACTA

Reverse	CGATGGTCAGGTCGATGTCATT

GSTA1 Mouse

Forward	CCGTGCTTCACTACTTCAAT
Reverse	GCATCCATGGGAGGCTTTCT

GR Mouse

Forward	TGCCTGCTCTGGGCCATT
Reverse	CTCCTCTGAAGAGGTAGGAT

Catalase Mouse

Forward	GACATGGTCTGGGACTTCTG
Reverse	GTAGGGACAGTTCACAGGTA

Prohibitin 1 Rat

Forward	TGGCGTTAGCGGTTACAGGAG
Reverse	GAGGATGCGTAGTGTGATGTTGAC

TNFα Rat

Forward	GCCTCTTCTCATTCCTGC
Reverse	CTTCTCCTCCTTGTTGGG

IL1β Rat

Forward	GCTAGGGAGCCCCCTTGTCGAG
Reverse	AGGCAGGGAGGGAAACACACGTT

IL6 Rat

Forward	TCCGCAAGAGACTTCCAGCCAG
Reverse	TGTGAAGTAGGGAAGGCAGTGGC

LC3b

Forward	CGATACAAGGGGGAGAAGCA
Reverse	ACTTCGGAGATGGGAGTGGA

Beclin-1

Forward	TGAATGAGGATGACAGTGAGCA
Reverse	CACCTGGTCTCCACACTCTTG

Lamp2a	
Forward	TGGCTAATGGCTCAGCTTTC
Reverse	ATGGGCACAAGGAGTTGTC
p62	
Forward	GGAGGAGCTCGAGCCATGGCGTTCACGGTGAA
Reverse	TATTATTTTTGGATCCTTCAATGGTGGAGGGTGTTCG

Table S2. Primary and Secondary Antibodies

Antibody	Concentration	Vendor (Cat. No)
Prohibitin 1	1:1000 (WB) 1:10 (ICC)	Abcam (ab28172)
Prohibitin 2	1µg/mL	Millipore (AB10198)
COX-IV	1µg/mL	Abcam (ab14744)
Alpha-Tubulin	1:5000	Abcam (7291)
TATA Binding Protein	1:2000	Abcam (ab818)
Beta-Actin	1:250	Abcam (ab8226)
NFκB-p65	1µg/mL	Abcam (ab16502)
Draq5®	1:1000 (ICC)	Cell Signaling (4084)
iNOS	1:500	Cell Signaling (2977)
Phospho-STAT3 Tyr705 (D3A7)	1:1000	Cell Signaling (9145)
Phospho-AKT (Ser473)(D9E)	1:2000	Cell Signaling (4060)
Pan-AKT (C67E7)	1:1000	Cell Signaling (4691)
DYKDDDDK Epitope Tag (Flag Epitope)	1:1000	Novus Biologicals (NBP1-06712)

FITC- Goat Anti Rat	1:50	Jackson ImmunoResearch Laboratories (112-095-003)
FITC-Donkey Anti Rabbit	1:50	Jackson ImmunoResearch Laboratories (711-095-152)
FITC-Donkey Anti Mouse	1:50	Jackson ImmunoResearch Laboratories (715-095-150)
HRP-Goat Anti Rabbit	1:7500	Bio-Rad (170-651)
Goat Anti-Rabbit IgG, DyLight™ 680 Conjugated	1:17000	Thermo Scientific (35568)
Goat Anti-Mouse IgG, DyLight™ 800 Conjugated	1:17,000	Thermo Scientific (35521)
Donkey Anti-Rabbit IRDye® 680	1:30,000	Li-Cor (926-32223)
Donkey Anti-Mouse IRDye® 800CW	1:30,000	Li-Cor (926-32212)
Goat Anti-Rat IRDye® 800CW	1:30,000	Li-Cor (926-32219)
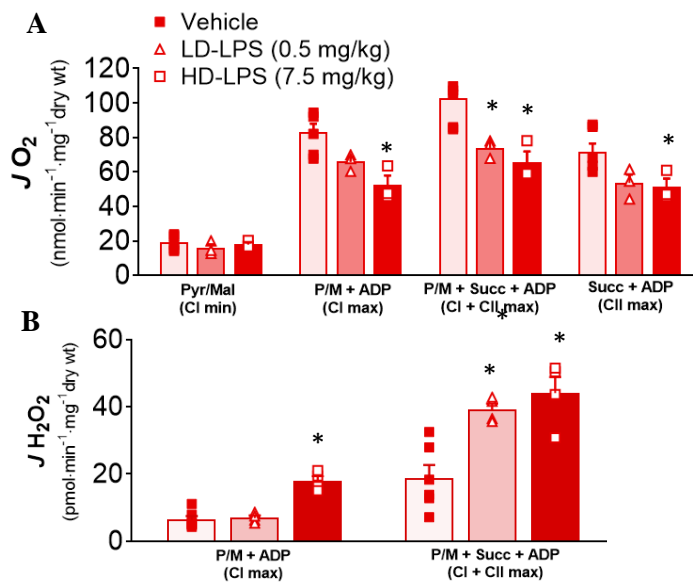
Figure S1. Functional abnormalities in cardiac mitochondria during endotoxemia. Endotoxemia was induced in Sprague-Dawley rats with both low-dose (0.5 mg/kg, LD) and high-dose LPS (7.5 mg/kg, HD), and mitochondrial respiratory flux was assessed in hearts dissected from the rats after 24 hours (**A**). O_2 consumption (JO_2) was assessed at baseline using pyruvate/malate alone (Pyr/Mal), and during maximal phosphorylating (i.e. ADP-stimulated) state with complex I (P/M_{ADP}), complex I and complex II substrate succinate ($P/M + S_{ADP}$) and complex II only (S_{ADP}) substrates. Mitochondrial H_2O_2 production/emission was also determined at timepoints indicated following LPS challenge with these substrates (**B**). N=4-5 rats per group. A two-tail Student's t-test was used to determine main effect of LPS versus vehicle control for each experiment.*P<0.05 vs Veh for each respective condition/endpoint. P/M= 5mM pyruvate/2mM malate; P/M_{ADP}= Pyr/Mal + 200 µM ADP; $P/M+S_{ADP}$ = Pyr/Mal + ADP + 5 mM succinate.
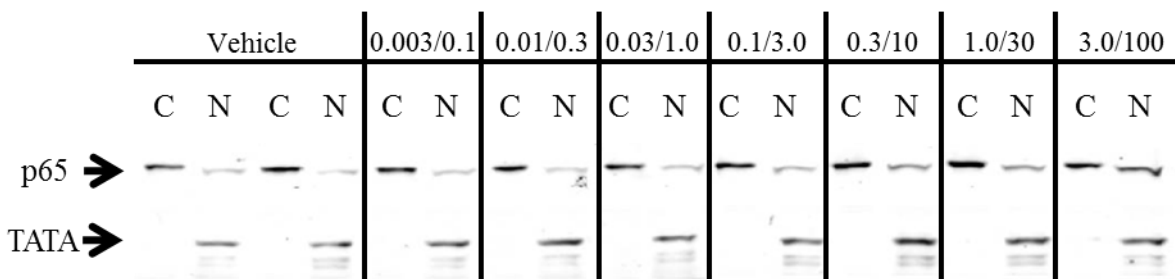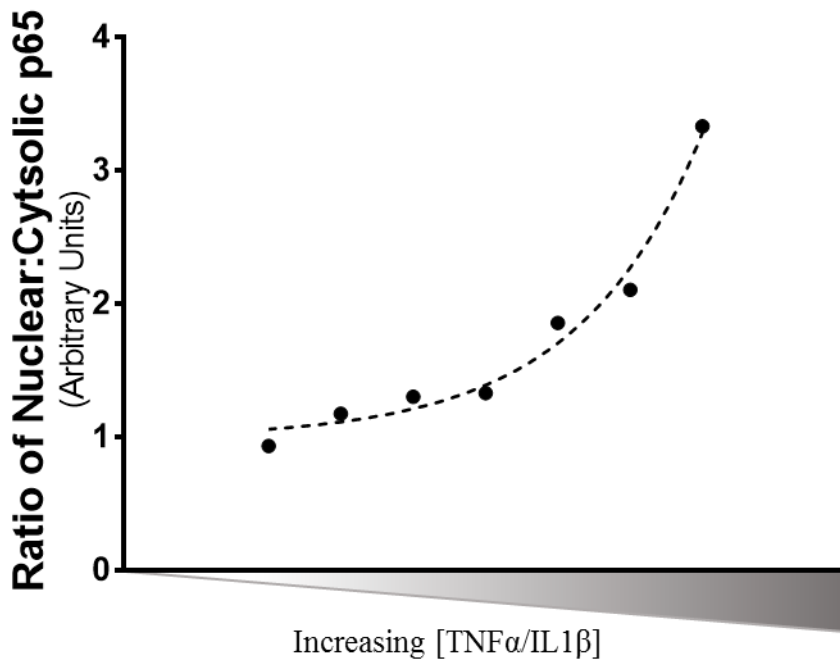
Figure S2. Establishing the 'sepsis-mimetic' model in HL-1 cardiomyocytes. Shown in the panels above are the effects of a dose-dependent increase in cytokines TNFα/IL1β on nuclear translocation of NFκB subunit p65 in the cells. Representative immunoblots showing cytosolic and nuclear p65 are shown in the bottom panel, while the densitometry results are displayed in the top panel. Maximal nuclear translocation was achieved at the 3.0/100 ng/mL doses, which is what was used for cell culture experiments in this study. The nuclear marker TATA-binding protein was used to confirm selectivity of the nuclear fraction.
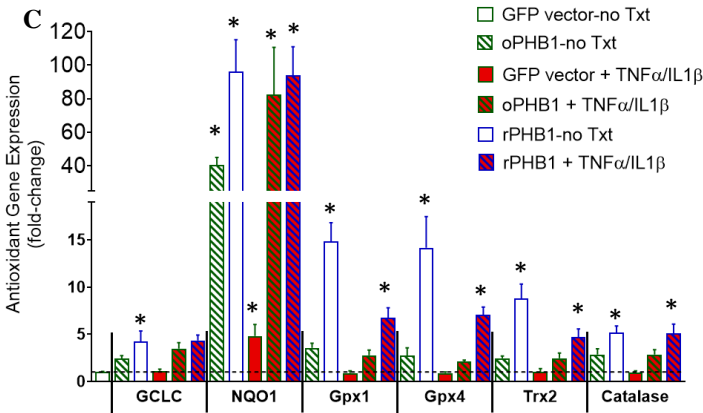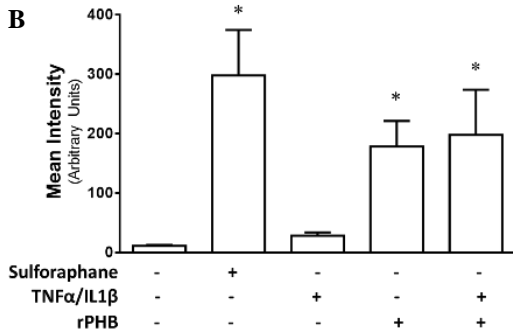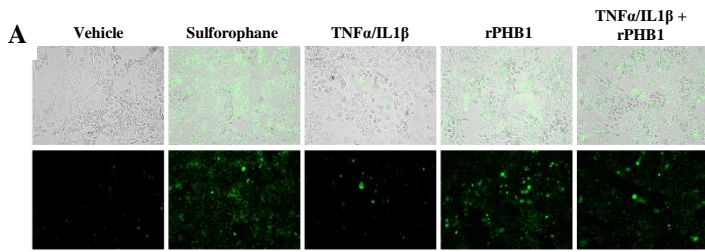
Figure S3. PHB1 upregulates antioxidant gene expression in HL1 cardiomyocytes. Cells were transiently transfected with plasmids encoding GFP under control of the antioxidant response element (ARE) promoter, and exposed to the various treatments as indicated in the representative image in (**A**), with quantification of the fluorescence intensities in (**B**). The effect of over-expressing PHB1 (oPHB1) and co-treatment with recombinant PHB1 (rPHB1) on antioxidant gene expression (**C**) is also shown. N=4 per group with technical replicates for each condition. A two-tail Student's t-test was used to determine main effect of LPS versus vehicle control for each endpoint indicated (fluorescence intensity or fold-change in mRNA). *P<0.05 vs control (GFP-vector, no treatment) for each respective endpoint. GCLC= glutamate-cysteine ligase catalytic subunit; NQO1=NADPH quinone oxidoreductase-1; Gpx=glutathione peroxidase; Trx=thioredoxin reductase-2
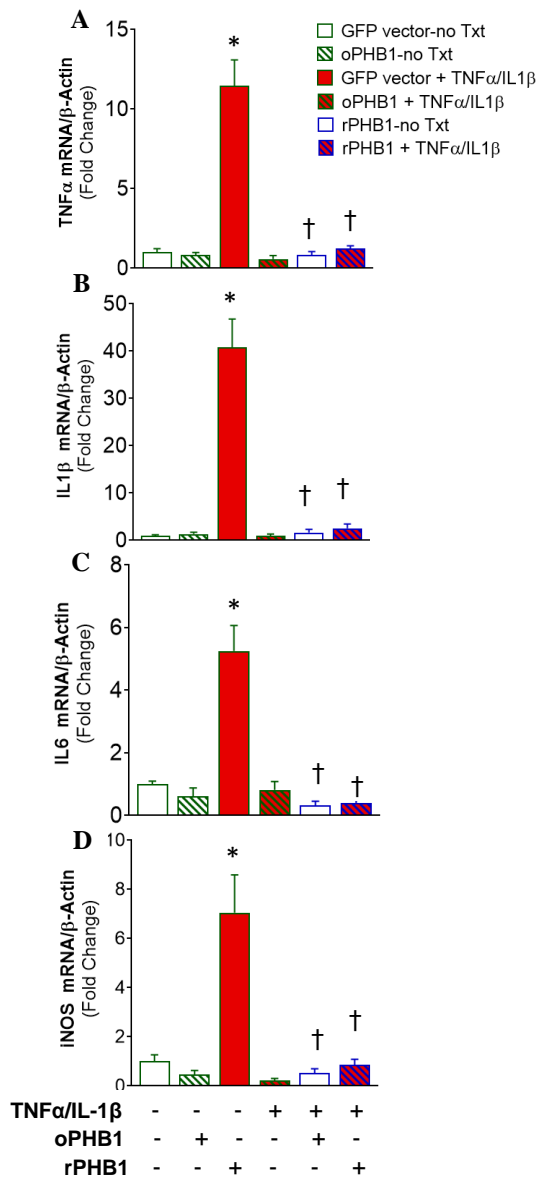
Figure S4. PHB1 suppresses inflammatory signaling in HL1 cardiomyocytes.
The effect of over-expressing PHB1 (oPHB) and co-treatment with recombinant PHB1
(rPHB) on inflammatory signaling in HL1 cardiomyocytes is shown above. Cells were
exposed to a sepsis-mimetic concentration of TNFα/IL1β for 24 hours, with or without
concomitant oPHB/rPHB1, and the expression of TNFα (A), IL1β (B), IL6 (C) and
iNOS (D) was measured. N=4 with technical replicates for each condition. A one-way
ANOVA followed by Neuman-Keuls post-hoc comparisons test between groups was
used to test for differences in main effect of treatment between groups. *P<0.0001 vs.
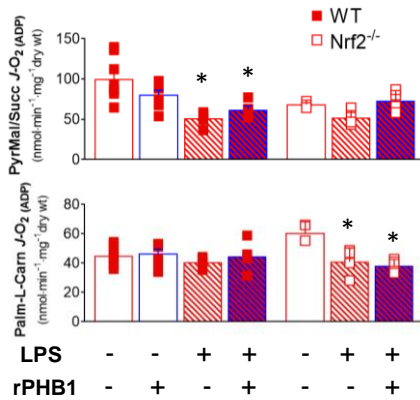untreated Control, †P<0.0001 vs. TNFα/IL1β treated.

Figure S5. Effect of rPHB1 treatment on mitochondrial respiration in WT and Nrf2-/- mice with endotoxemia. Mitochondrial respiratory flux (JO_2) was assessed in permeabilized ventricular myofibers in the presence of 200 μM ADP (clamped with saturated glucose/hexokinase in respiration medium). Respiration was supported by 5 mM pyruvate, 2 mM malate, and 5 mM succinate (top panel), and 100 μM palmitoyl-L-carnitine + 2 mM malate (bottom panel). N=4-5 mice per group. A one-way ANOVA followed by Neuman-Keuls post-hoc comparisons test between groups was used to test for differences in main effect of treatment between groups. *P<0.05 vs. vehicle-treated mice for that respective genotype.
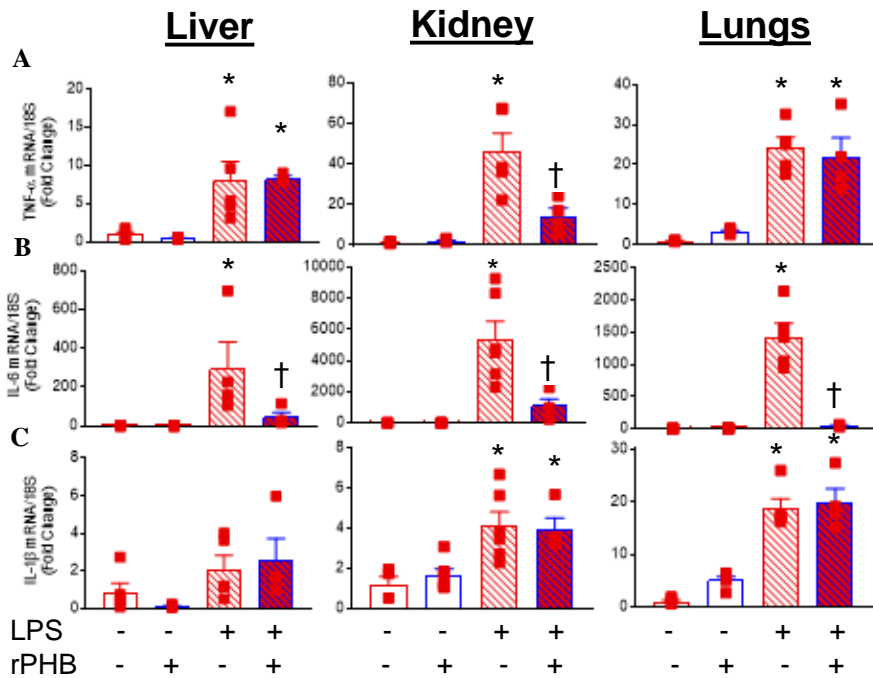
Figure S6. Effect of rPHB1 treatment on inflammatory cytokine expression in liver, kidney and lungs from WT mice with endotoxemia. Expression of cytokines TNFα (**A**), IL-6 (**B**) and IL-1β (**C**) were measured with qRT-PCR in liver, kidney and lung tissue from WT mice at 16 hrs following LPS challenge, with and without rPHB1 treatment (3 doses of 300 ng rPHB1, i.p.,, as shown in Figure 4). N=4-5 mice per group. A one-way ANOVA followed by Neuman-Keuls post-hoc comparisons test between groups was used to test for differences in main effect of treatment between groups. *P<0.05 vs. vehicle-treated mice, †P<0.0001 vs. LPS only, for that respective tissue.
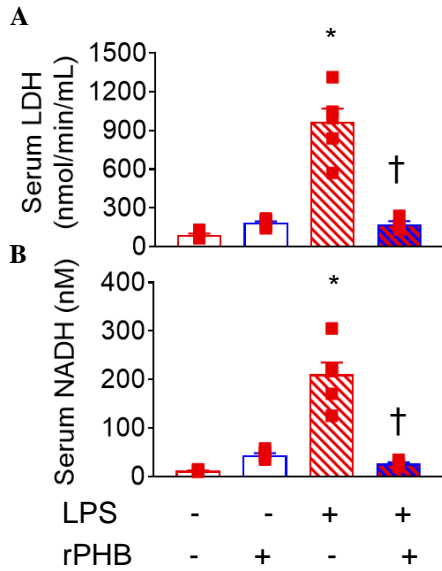
A

Serum LDH (nmol/min/mL)

B

Serum NADH (nM)

| LPS | - | - | + | + |
| rPHB | - | + | - | + |

Figure S7. Effect of rPHB1 treatment on serum markers of tissue necrosis in WT mice with endotoxemia. Tissue necrosis markers lactate dehydrogenase (LDH) (**A**), and NADH (**B**) were measured in serum obtained from WT mice at 16 hrs following LPS challenge, with and without rPHB1 treatment (3 doses of 300 ng rPHB1, i.p.,, as shown in Figure 4A). N=4 mice per group. A one-way ANOVA followed by Neuman-Keuls post-hoc comparisons test between groups was used to test for differences in main effect of treatment between groups. *P<0.05 vs. vehicle-treated mice, †P<0.0001 vs. LPS only.
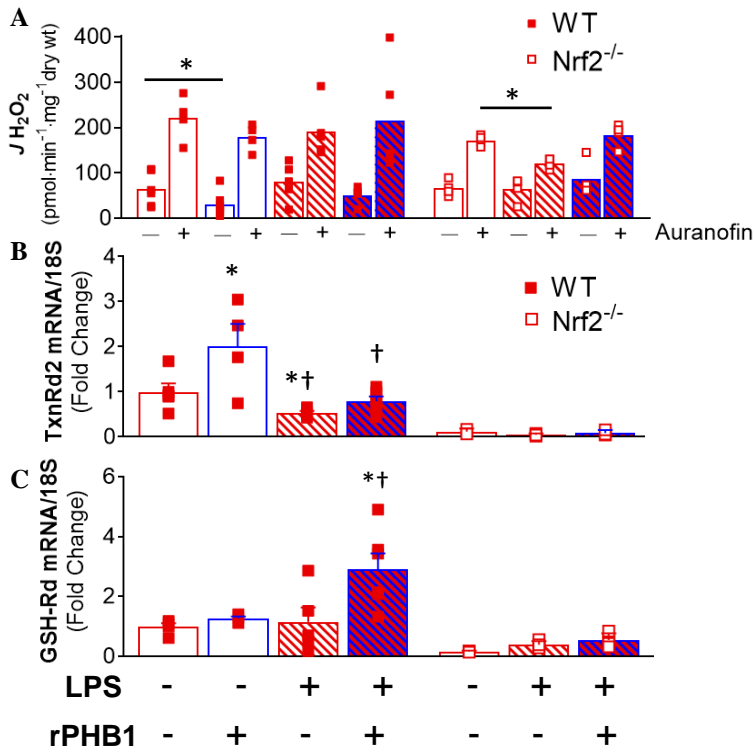
Figure S8. rPHB1 normalizes mitochondrial redox balance and augments antioxidant gene expression in heart during endotoxemia. The effect of rPHB1 treatment on mitochondrial H_2O_2 production/emission (**A**) in the presence and absence of thioredoxin reductase inhibitor Auranofin is shown in permeabilized ventricular myofibers prepared from the mice at the terminal stage of the experiment (16 hours post-LPS, after 3 doses of rPHB1). Expression of TxnRd2 (B) and glutathione reductase (C) is also shown. N=4-5 mice per group. A one-way ANOVA followed by Neuman-Keuls post-hoc comparisons test between groups was used to test for differences in main effect of treatment between groups in each experiment.*P<0.05 vs. untreated mice (Vehicle), for that respective time-point and genotype, †P<0.01 vs. LPS only, for that respective genotype.
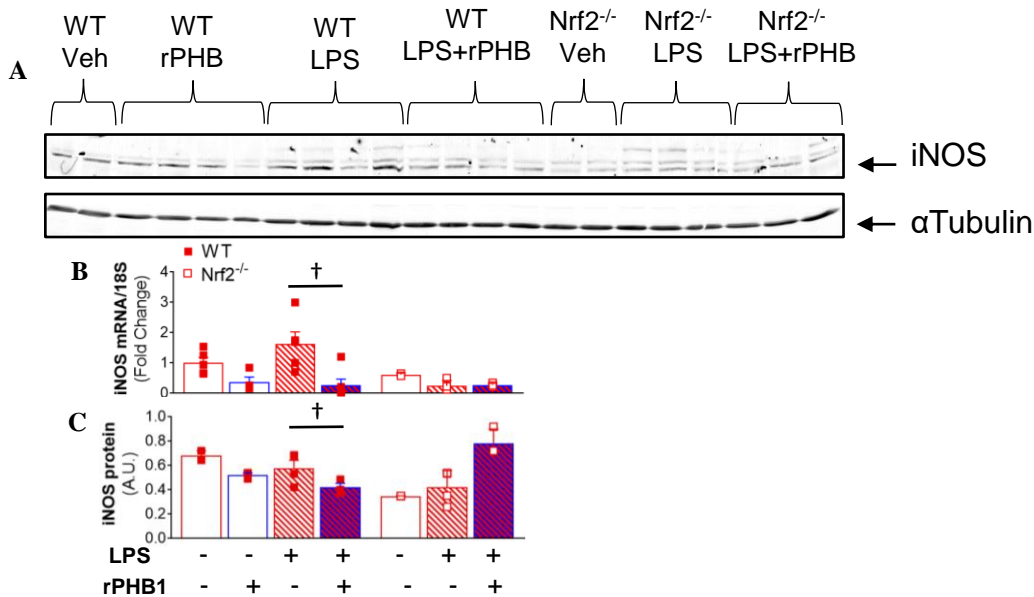
Figure S9. Effect of rPHB1 treatment on cardiac iNOS in WT and Nrf2-/- mice with endotoxemia. The effect of rPHB1 treatment on iNOS expression and content are shown at both the whole protein level (**A, C**) and mRNA (**B**) in WT and Nrf2-/- mice at 16 hrs following LPS challenge, with and without rPHB1 treatment (3 doses of 300 ng rPHB1, i.p.,, as shown in Figure 4). N=3 mice per group. A one-way ANOVA followed by Neuman-Keuls post-hoc comparisons test between groups was used to test for differences in main effect of treatment between groups. †P<0.01 vs. LPS only.